UNIVERSIDADE DE LISBOA
FACULDADE DE CIÊNCIAS
DEPARTAMENTO BIOLOGIA VEGETAL

Development of New Cellular Models for Step-by-Step Analysis of Astrogliogenic Pathways

Mestrado em Biologia Molecular e Genética

Ana Catarina Maia Rocha

Dissertação orientada por:
Dr. Federico Herrera
Dr. Margarida Gama Carvalho

2015

Dedicated to my best friend Ana Patricia Justino Duarte.

Your light will forever shine throughout the universe.

Especially in those who love you.

ACKNOWLEDGEMENTS

I would like to express my gratitude to all of those involved in the development of this thesis.

To my supervisor Federico Herrera, who provided me the opportunity to work in his laboratory, as well as for the dedication and patience for the development of this work. Thank you for all the dedicated time and transmission of knowledge, which encouraged my scientific growth.

To my co-supervisor Margarida Gama-Carvalho for her support and avid availability to always enlighten me.

To Dr. Mariana Santa-Marta for all the help and know-how in several scientific techniques and for the constructive criticism that helped me to improved my technical abilities and critical spirit.

To Dr. Isabel Pacheco for all the support in the laboratory and clarifying personal and scientific talks.

To the Unit of Imaging and Cytometry at IGC for all the technical support and prompt availability.

A special thanks to my boyfriend, Diogo Mateus, who relentlessly supported and inspire me to continue working hard and appreciate the bright side of life.

Last but not least, an enormous thanks to my family and friends for the unlimited support and care, without them this thesis would have never been accomplished. A special thanks to my friends Flávia Santo and Susana Mendonça for their unconditional support, scientific discussions and lay down times.

ABSTRACT

The Janus kinase/signal transducers and activators of transcription (JAK/STAT) pathway is an evolutionarily conserved mechanism for signalling transduction and involves four steps regulated by protein-protein interactions. Cytokines bind to the common receptor glycoprotein 130 (gp130) to activate JAKs, which then phosphorylate STATs leading to its dimerization and translocation to the nucleus to induce target genes.

The activation of this pathway is essential for astroglia production during brain development and upon central nervous system (CNS) damage. Astrocytes are crucial to neuronal survival and determine the ability of the CNS to repair damage and regenerate. Multiple brain insults elicit a reactive response from astrocytes called astrogliosis, which can impair axonal regeneration and the reestablishment of the neural circuits. Due to the pleiotropic effects of the JAK/STAT pathway several attempts have been made to target this signalling pathway. However, further investigation on protein interactions and dynamics are required for an efficient determination of molecular targets. In this regard, bimolecular fluorescence complementation (BiFC) assays offer a direct method to identify potential modulators of protein interactions.

In this study, we developed two Venus-based BiFC systems to screen for modulators of key protein-protein interactions in the JAK/STAT pathway, a gp130-Venus and a Venus-STAT3 BiFC system. Both systems worked in living cells and displayed a similar behaviour to endogenous proteins sustaining novel information regarding the dimerization of these proteins. The Venus-STAT3 BiFC system was further validated by a specific inhibitor of STAT3. These results show the potential of the BiFC systems as tools for drug and genetic screenings, as well as step-by-step analysis of the JAK/STAT pathway in diverse biological contexts.

Keywords: JAK/STAT pathway; gp130; STAT3; astrocytes; BiFC system.

RESUMO

A via de sinalização JAK/STAT é um mecanismo de transdução de sinal conservado na evolução, que envolve quatro etapas de fosforilação e a formação de vários complexos proteicos. As citocinas da família da interleucina 6 ligam-se à cadeia comum do receptor composta pela glicoproteína 130 (gp130), induzindo uma alteração de conformação que ativa as JAKs, construtivamente associadas a estes. Por sua vez, as JAKs fosforilam resíduos de tirosina específicos nos recetores que permitem recrutar proteínas, como o fator de transcrição STAT3. As JAKs fosforilam o STAT3 em resíduos específicos e estes dímeros ativados migram para o núcleo para induzir a transcrição de genes específicos. A fosforilação do STAT3 pelas JAKs sempre foi considerada o processo pelo qual estes fatores de transcrição dimerizam, migram para o núcleo e ligam-se ao DNA. No entanto, estudos recentes demonstram que esta proteína existe como dímeros estáveis *a priori* e estes são continuamente transportados entre o citoplasma e o núcleo.

A ativação deste mecanismo de transdução de sinal é essencial para a produção de astrócitos durante o desenvolvimento do cérebro e em alturas de dano no sistema nervoso central. Os astrócitos são extremamente importantes para a sobrevivência dos neurónios e determinam a capacidade de o sistema nervoso central reparar danos e de se regenerar. Existem múltiplos estímulos negativos que podem gerar uma resposta reativa dos astrócitos, denominada astrogliose, que é mediada pela via JAK/STAT. Quando o grau de lesão é severo os astrócitos formam a cicatriz glial, que constitui uma barreira entre o microambiente lesado e o parênquima saudável. Esta barreira limita a extensão do dano e inflamação provenientes do estímulo patológico, protegendo as células neuronais. No entanto, esta resposta imediatamente protetora pode promover doenças e inibir a regeneração do sistema nervoso central se o estimulo patológico persistir e a astrogliose for incapaz de o resolver.

A via JAK/STAT condiciona inúmeras respostas biológicas envolvidas no ciclo celular, diferenciação e migração celular e apoptose. Devido ao seu largo espectro de ação, esta via está envolvida em processos fisiológicos fundamentais, como por exemplo, o desenvolvimento e a hematopoiese. A sua associação a diversas patologias é inerente às suas funções, e estas incluem inflamação crónica, doenças autoimunes, desordens neurodegenerativas e vários tipos de cancro. A ativação constitutiva do fator de transcrição STAT3 está associada a muitas destas patologias tornando esta via num alvo terapêutico promissor. No entanto, é necessário um maior conhecimento relativamente às dinâmicas intervenientes em interações proteicas subjacentes a este mecanismo, de forma a determinar mais eficientemente possíveis alvos moleculares e os seus moduladores.

A complementação de fluorescência bimolecular (BiFC) é uma técnica que permite visualizar interações proteicas em células vivas. Esta técnica baseia-se na fusão de fragmentos complementares de uma proteína fluorescente com as proteínas de interesse. Quando as proteínas de interesse

interagem a proteína repórter é reconstituída e emite um sinal fluorescente proporcional ao número de dímeros formados. Este sinal pode ser analisado, quantitativamente e qualitativamente, utilizando métodos convencionais como a citometria de fluxo e a microscopia de fluorescência. O sistema BiFC também permite uma análise direta para identificar moduladores promissores de interações protéicas. Aplicando este sistema ao estudo da via JAK/STAT, teremos uma maior compreensão sobre as complexas interações protéicas que controlam a astrogliose, promovendo a regeneração do sistema nervoso central.

No presente estudo foram desenvolvidos dois sistemas de BiFC baseados na proteína fluorescente Venus, de forma a avaliar moduladores na interação de proteínas cruciais na via JAK/STAT. Estes sistemas, gp130-Venus e Venus-STAT3, foram criados por clonagem molecular a partir de outros plasmídeos. Posteriormente foram testados em células animais e analisados por citometria de fluxo e microscopia de fluorescência de forma a avaliar a sua funcionalidade, eficiência e comportamento.

Tanto o sistema gp130-Venus como o Venus-STAT3, funcionaram em células vivas, tendo o primeiro baixos níveis de fluorescência, enquanto que o segundo demonstrou uma eficiência total superior. O comportamento de ambos os sistemas foi similar às proteínas endógenas, confirmando as investigações recentes referentes ao estado de dimerização destas proteínas na ausência de estímulos. O Venus-STAT3 produziu um maior nível de fluorescência e portanto foi o sistema estudado com mais profundidade.

Para aferir a aplicabilidade do sistema molecular desenvolvido no estudo de interações de proteína, estudámos um dos plasmídeos do sistema Venus-STAT3 em combinação com outros plasmídeos que continham a metade complementar da proteína Venus. Os plasmídeos analisados eram constituídos por diversas proteínas envolvidas em doenças neurodegenerativas como: *huntingtin*, *tau*, *synuclein*, DJ-1 e GFAP, e tanto o factor de transcrição p53 como o seu regulador, mdm2. O sistema Venus-STAT3 também foi investigado em células animais após estimulação com citocinas, voltando a verificar-se um comportamento semelhante ao endógeno.

O sistema Venus-STAT3 confere informação direta sobre a dimerização de STAT3. Para provar o seu potencial como ferramenta para a descoberta de novos moduladores desta interação, foi testado com um inibidor específico de dimerização recentemente desenvolvido pelo grupo de investigação da Dr. Rita Delgado. O tratamento com este inibidor reduziu a fluorescência gerada pela interação dos dímeros STAT3, voltando-se a validar este sistema.

Os resultados apresentados demonstram o potencial destes sistemas BiFC a dois níveis: 1) como ferramentas na análise de moduladores farmacológicos e genéticos, e 2) na dissecção dos intervenientes da via JAK/STAT em diversos contextos biológicos. Estas ferramentas contribuem para um maior conhecimento das dinâmicas das interações proteicas envolvidas nesta cascada de

sinalização, que mesmo parecendo simples se torna complexa quando analisada em conjunto com outras vias de sinalização.

Palavras-chave: via JAK/STAT; gp130; STAT3; astrócito; sistema BiFC.

GENERAL CONTENTS

INDEX OF IMAGES

LIST OF ABBREVIATIONS

ALDH1L1	Aldehyde dehydrogenase 1 family member L1
AQ4	Aquaporin 4
Bcl-2	B-cell lymphoma 2
Bcl-xL	B-cell lymphoma-extra large
BiFC	Bimolecular fluorescence complementation
BMP	Bone morphogenic proteins
BSA	Bovine serum albumin
CBP	CREB binding protein
CLC	Cardiotrophin-like cytokine
CNS	Central Nervous System
CNTF	Ciliary neurotrophic factor
CT-1	Cardiotrophin-1
DCX	Doublecortin
DMEM	Dulbecco's Modified Eagle's Medium
EAA1/2	Excitatory amino acids transporters ½
EMSA	Electrophoretic mobility shift assay
FBS	Fetal bovine serum
GAPDH	Glyceraldehyde-3-phosphate dehydrogenase
GFAP	Glial fibrillary acidic protein
Gp130	Glycoprotein 130
HEK293	Human Embryonic Kidney cells
Hes	Homologue of hairy and enhancer of split
HRP	Horseradish peroxidase
Htt	Huntingtin
JAK	Janus kinase
LIF	Leukemia inhibitory factor
LIFR	Leukemia inhibitory factor receptor
MAPK	Mitogen-activated protein kinase
Mcl-1	Myeloid cell leukemia 1
OSM	Oncostatin M
OSMR	Oncostatin M receptor
P/S	Penicillin/Streptomycin solution
PBS	Phosphate buffered saline

PI3K	Phosphoinositide 3-kinase
PIAS	Protein inhibitors of activated STATs
PTPs	Protein tyrosine phosphatases
SDS	Sodium dodecyl sulphate
Ser	Serine
SH2	Scr homoly 2
SOCS	Suppressor of cytokine signalling
STAT	Signal transducer of activators of transcription
TBE	Tris-borate-EDTA
TBST	Tris-buffered Saline Tween 20
TGF-β	Transforming growth factor beta
Tyr	Tyrosine
V1	Venus 1
V2	Venus 2
WB	Western Blot
YFP	Yellow fluorescent protein
α-syn	α-synuclein

Introduction

1.1 The JAK/STAT Pathway

Each biological process is uniquely regulated by a series of biochemical mechanisms that derived from complex cascades of protein-protein interactions. The Janus kinase (JAK)/Signal transducer and activators of transcription (STAT) pathway is an evolutionarily conserved mechanism by means of which extracellular factors control gene expression. This signalling pathway plays a relevant role in a wide range of phenomena, both physiological and pathological, as it is involved in embryonic development, neuronal regeneration, acute-phase response to injury, neurodegeneration and cancer, to mention just a few examples.

The consensus JAK/STAT pathway is relatively straightforward and comprises four key phosphorylation steps and the formation of several protein complexes at the membrane, cytoplasm and nucleus (Figure 1). Upon ligand binding to receptor glycoprotein 130 (gp130) homo/heterodimers [1], JAKs become activated by transphosphorylation due to close proximity [2][1]. JAKs then phosphorylate specific conserved tyrosine residues within the cytoplasmic part of the receptor [3]. These residues act as docking sites for signalling molecules containing Scr homology 2 (SH2) domains. STAT3 proteins are recruited by their SH2 domains to these sites, where JAKs phosphorylate them in specific tyrosine and serine residues (Tyr705 and Ser727) [4]. This leads to the release of phosphorylated STAT3 dimers from the receptor [5] and their translocation into the nucleus, where they bind to specific promoter regions to induce gene expression. Activated STAT3 dimers can partner with coactivators, such as p300/CREB binding protein[2] (CBP) or Smad[3–6] proteins, to enhance the transcriptional rate of target genes[7], such as the glial fibrillary acidic protein (GFAP) [6].

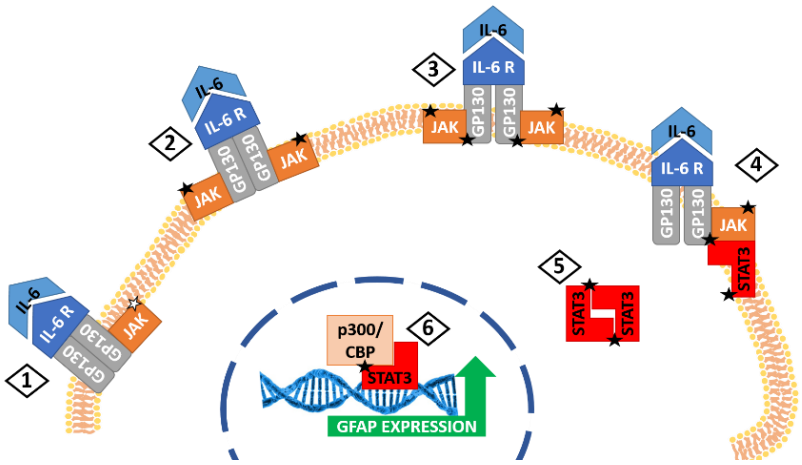

Figure 1 – Schematic representation of the JAK/STAT pathway. [1] Ligand binding to receptor complex. [2] Phosphorylation of JAKs. [3] JAKs phosphorylate specific tyrosine residues in the receptor. [4] Recruitment of STAT3 to the receptor and subsequently phosphorylation by JAKs. [5] Activated STAT3 dimers are released from the receptor. [6] STAT3 dimers translocate to the nucleus, associate with co-activators and induce expression of target genes (e.g. GFAP).

The IL-6 family of cytokines is the main stimulator of this pathway[1], enclosing IL-6[8], IL-11[9], LIF (leukemia inhibitory factor), OSM (Oncostatin M), CNTF (ciliary neurotrophic factor), CT-1 (cardiotrophin-1) and CLC (cardiotrophin-like cytokine). The interaction between different IL-6 cytokines and their receptors and effector molecules is specific, eliciting precise as well as overlapping physiological responses[10,11] (Figure 2). Cytokines bind to plasma membrane receptor complexes containing the common signal transduction receptor chain gp130, which can form homodimers or heterodimers with LIF receptor or OSM receptor. IL-6, IL-11 and CNTF first bind specifically to their non-signalling α-receptors (IL-6Rα, IL-11Rα and CNTFRα)[12,13]. They are then able to efficiently recruit the gp130 signalling receptor subunits or induce a conformational change in transient homodimers of gp130[14,15]. The remaining cytokines signal via heterodimers of either gp130/LIFR (LIF, CNTF, CT-1 and CLC) or gp130/OSMR (OSM)[1,16].

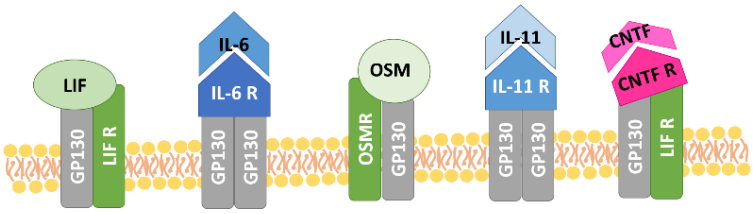

Figure 2 – Different cytokines and receptor complexes can trigger the JAK/STAT pathway.

Phosphorylation of STATs by JAKs is the next step in the pathway. Although the STAT family has 7 members in humans, we will focus on STAT3 because it is the key effector of astrogliogenesis and central to this thesis. The consensus for this pathway is that STAT3 phosphorylation by JAKs leads to STAT3 dimerization, subsequent translocation into the nucleus and binding to DNA[17]. However, current evidence strongly indicates that STAT3 exists as stable homodimer prior to cytokine stimulation and that Ty705 phosphorylation changes its conformation[18,19]. These dimers shuttle continuously between the cytosol and the nucleus in unstimulated cells, suggesting that stimulated cells decrease STAT3 nuclear export and retains it in the nucleus[20–22]. Although unphosphorylated dimers exist and are present in the nucleus, they are incapable of binding to specific promoter regions of active STAT3[18]. Unphosphorylated dimers are involved in chromatin remodelling and transcription of MET, MRAS and cyclin D1 by cooperating with other protein complexes such as NFκB and CD44[23–25].

The JAK/STAT pathway is tightly regulated by genetic inhibitors at different levels. Protein tyrosine phosphatases (PTPs) bind to JAKs and STAT3 to facilitate their dephosphorylation[26]. The suppressor of cytokine signalling (SOCS1/3) binds to JAKs via its SH2 domain and abolishes STAT3 recruitment to the receptor[27]. Finally, protein inhibitors of activated STATs (PIAS) obstruct STAT3 DNA binding ability and induce the expression of corepressors[27].

1.2 The JAK/STAT Pathway Is a Promising Therapeutic Target

The JAK/STAT pathway is essential for normal development and physiology. Mice deficient in one of the members of the IL-6 family show mild phenotypes due to the pleiotropic activities of gp130-dependent cytokines. In contrast, gp130-null mice die 12.5 days post-coitum, exhibiting disrupted placental architecture, hypoplastic development and a decrease in fetal liver hematopoiesis. Gp130 mutations produce defects in multiple organs (e.g. brain, heart, liver and lungs)[28]. Both gp130- and LIFR-deficient mice exhibit a significant reduction of astrocytes and GFAP expression, as well as loss of motor and sensory neurons in several loci at late stages of development[29]. Knockout mice for JAK1 or JAK2 are not viable, dying in the perinatal and embryonic period, respectively. Knockout models for STAT proteins are viable except for STAT3 -/- mice, which shows severe developmental abnormalities, highlighting the relevance of this transcription factor[30].

The wide range of effects of the JAK/STAT pathway in biological processes is mainly due to activated STAT3 target genes. These are related to cell cycle control (e.g. c-Myc); apoptosis (e.g. Bcl-xL, Bcl-2, Mcl-1 and surviving); astrocyte differentiation and development (e.g. GFAP and S100); and metastasis (e.g. metalloproteases and vascular endothelial growth factor), which have been associated with the onset and progression of a number of diseases[31]. These include chronic inflammatory responses[32], autoimmune disorders[33,34], neurodegenerative disorders[35,36] and cancers[37–39].

In many of these disorders, STAT3 is continuously activated by dysregulation of upstream kinases or loss of endogenous inhibitors. Several therapeutic approaches attempted to suppress constitutive activation of STAT3. For instance, the AG490 compound inhibits JAK phosphorylation and subsequently STAT3 phosphorylation, reducing invasion and adhesion of highly metastatic cells[40]. Other JAK inhibitors have demonstrated clinical efficiency in rheumatoid arthritis and other inflammatory diseases[34].

Although, there is an increasing interest in modulating this pathway, little is still known about its time-spatial interactions with other signalling pathways that modulate the final outcome of JAK/STAT activation (Figure 3). These pathways can induce the formation of co-activator complexes with STAT3 (e.g. transforming growth factor beta superfamily[3,41] [TGF-β] and retinoic acid[5,42–44] [RA]), potentiate Ser727 phosphorylation (e.g. Ras/mitogen-activated protein kinase[45,46] [MAPK] and phosphoinositide 3-kinase[5,44,47] [PI3K]), or facilitate STAT3 phosphorylation by JAKs (Notch pathway[48,49]).

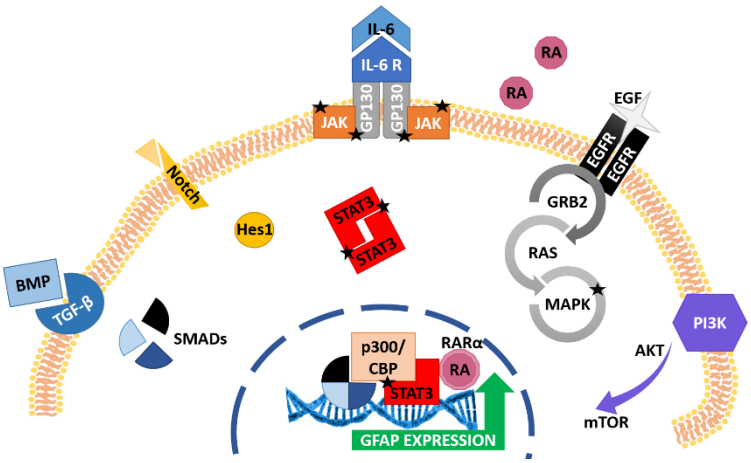

Figure 3 – Representative scheme of multiple signalling cascades interacting with the JAK/STAT pathway to induce STAT3 gene expression. From left to right: TGF-β superfamily, Notch, JAK/STAT, Retinoic Acid, Ras/MAPK and PI3K pathway.

Understanding the interplay between the JAK/STAT pathway and other pathways will contribute to a better comprehension of its biological consequences in human pathology, allowing the discovery of new modulators and unlocking a broader spectrum of molecular targets for future therapeutics.

We are especially interested in the role of the JAK/STAT pathway in the production of astroglia during brain development and upon CNS damage, which determines the ability of the CNS to repair damage and regenerate.

1.3 Astrocytes Are an Essential Cell Type in the Brain

1.3.1 Astrocytes: History, Definition and Classification

In the end of the 19th century, Rudolph Virchow coined the term Neuroglia for the once thought inactive connective tissue that supported neurons in the Central Nervous System (CNS). The development of metallic staining techniques by Camilo Golgi, Santiago Ramón y Cajal and Pío del Rio-Hortega enabled the discovery of three non-excitable neural cell types: astrocytes, oligodendrocytes and microglia. All three are crucial for neuronal function, but for the purpose of this work only astrocytes will be further reviewed.

The word astrocyte is derived from the Latin and Greek expression “astra” and “kytos”, and literally means star-shaped cell. Astrocytes are the most abundant cell in the brain (excluding cerebellum) in an overall proportion of 5:1 versus neurons. These cells are classified by their morphology and presence in white matter (fibrous astrocytes), or grey matter (protoplasmic astrocytes) (Figure 4).

The majority of fibrous astrocytes display several long intersecting processes[50], rich in intermediate filaments that radiate symmetrically from the cell soma. These processes do not frequently branch, but they extend along axons bundles providing structural support for axonal tracts and commonly forming end feet at capillaries and nodes of Ranvier. On the other hand, protoplasmic

astrocytes have a complex morphology with highly branched processes that enfold neuronal synapses and cell bodies by forming membranous sheets. This subtype has fewer intermediate filaments but a higher density of organelles. Protoplasmic astrocytes also interact with capillaries and the pial surface[51]. This subtype is organized in individual non-overlapping anatomical domains that are free of processes from any other astrocytes[50].

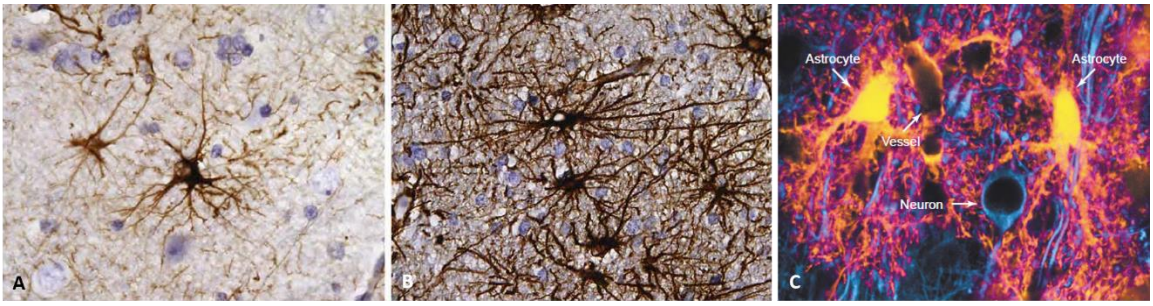

Figure 4 – Astrocytes are star-shaped cells. A) and B) Protoplasmic and fibrous human astrocytes stained for GFAP (brown) with haematoxylin counterstain, respectively. [Adapted from Rao, A & Jacobson, M, 2005, Development Neurobiology, 4th edn, Plenum Publishers, New York] C) Spatial organization of astrocytes (yellow) and neurons (blue) in rat cortex. A small vessel is outlined by astrocytic endfeet. [Adapted from Nedergaard, M., Ransom, B. & Goldman, S. a. New roles for astrocytes: redefining the functional architecture of the brain. Trends Neurosci. 26, 523–30 (2003)]

Astrocytes integrate a syncytial superstructure through evenly distributed gap junctions along their processes[52]. This network enables fast communication between cells, because they are permeable to ions and other biologically important molecules (e.g. nucleotides, sugars, amino acids). Glial excitability through the release of calcium also allows astrocytes to gather information from the extracellular space. These mechanisms allow a rapid and coordinated regulation of the electrical and biochemical demands of the tissue.

From a more molecular point of view, astrocytes are mainly characterized by the expression of the intermediate filament GFAP, the calcium binding protein S100β and glutamine synthetase[53]. Other markers include the glutamate transporters GLAST and GLT-1 in rodents, which correspond to excitatory amino acids transporters 1 and 2 (EAA1, 2) in the human brain; the water channel aquaporin 4 (AQ4), connexin 43 (gap junctions); and the aldehyde dehydrogenase 1 family, member L1 (ALDH1L1), a selective label for cortical astrocytes *in vivo*[54,55].

1.3.2 Astrocytes Maintain Normal Neuronal Function and Survival

Astrocytes were initially regarded as secondary cells of the CNS, only providing a structural support for neurons. Over the past decade, numerous studies have come forward to demystify this housekeeping view of astrocytes, picturing a more active and dynamic role for them in normal brain function.

One of the best recognized features of astrocytes is their dense expression of potassium (K+) channels. This enables an efficient regulation of physiological pH by removing the excess of extracellular K+ produced during normal and pathological neuronal activity[56]. The water channel AQ4

is enriched in astroglial processes, where it regulates fluid homeostasis and facilitates the flux of gases by contact with blood vessels[56]. Furthermore, astrocytes are the main responsible for the inactivation and recycling of glutamate due to their specific expression of glutamate transporters and glutamine synthetase[53]. Glutamate is the main excitatory neurotransmitter in the brain, but it can also be a powerful neurotoxin at high concentrations. Astrocytes remove 80% of extracellular glutamate by EAAT1/2 transporters, preventing their potentially detrimental accumulation. Astrocytes also produce and secrete glutathione to the extracellular medium, and thus provide antioxidant protection and reduce neuronal toxicity[50]. Besides providing a healthy environment, these star-shaped cells release energy metabolites to support neuron activity, which facilitates learning and memory[36].

Astrocytes are closely associated with neuronal membranes and specifically with synaptic regions, by enwrapping presynaptic and postsynaptic terminals. Neurons co-cultured with astrocytes developed seven-fold more mature functional synapses than neurons grown in the absence of astrocytes[57,58]. These cells also regulate postsynaptic currents though calcium excitability by releasing neuroactive molecules, which influences long-term potentiation and synaptic scaling[57]. Very importantly, the interaction of astrocytes, perycites and vascular endothelial cells form the blood-brain barrier and regulate CNS blood flow in response to neuronal activity[36,56].

1.3.3 Astrocytes a Major Line of Defence Against Brain Insults

Astrocytes protect the brain tissue from numerous pathological stimuli, from acute lesions, such as trauma or stroke, to chronic neurodegeneration, such as Alzheimer and Parkinson diseases. A common hallmark of these disturbances is the proliferation and hypertrophy of astrocytes in response to insults, a phenomenon known as reactive astrogliosis[50,59].

Astrogliosis can range from mild to severe with glial scar formation[56]. Upregulation of GFAP expression and other genes leads to hypertrophy of the cell body and processes. However, astrocytes will only invade each other´s domain when the tissue is severely damaged. If the blood-brain barrier is disrupted, the domain network organization is dismantled and astrocytes proliferate and form a dense web of interdigitated processes and cell bodies, known as the glial scar[59–61] (Figure 5). Reactive astrocytes express pro-inflammatory cytokines and trophic factors that alter the microenvironment[62]. Furthermore, they also produce dense extracellular deposits of proteoglycans and other molecules capable of remodelling the local extracellular matrix, including collagen, chondroitin sulfate proteoglycans and tenascin-C, among others[50,60].

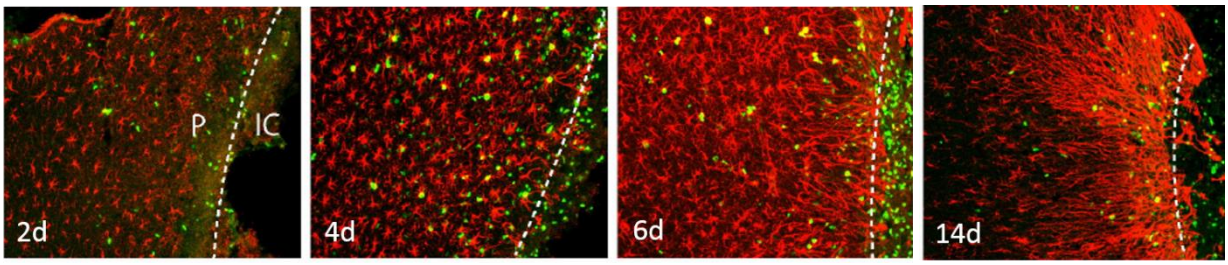

Figure 5 - Confocal images of GFAP and BrdU expression demonstrating astrocyte reactivity after photothrombosis. Astrocyte proliferation starts by day 2, lost of individual domain is apparent by day 6 and a glial scar is formed by migrating astrocytes by day 14. [Adapted from Choudhury, G.R., Ding,S., Reactive astrocytes and therapeutic potential in focal ischemic stroke, Neurobiol.Dis. (2015)[61]]

The reactivity of astrocytes can be triggered by any lesion involving the CNS, such as neuroinflammation, necrosis, edema, infection or chronic neurodegeneration. The occurrence of these processes leads to the upregulation of STAT3 in reactive astrocytes, which is essential for neuroprotection in acute responses[63–65]. Production of cytokines from the IL-6 family in response to brain insults protects motor neurons of the spinal cord from degeneration following spinal cord injury in adult mice[62]. Absence of SOCS3 promotes gp130-mediated CNTF signalling, promoting axon regeneration[66,67]. Deletion of STAT3 following traumatic insults leads to limited migration of astrocytes. This has been associated with widespread infiltration of inflammatory cells, demyelination and severe loss of motor function[68]. STAT3 activation induces the expression of anti-apoptotic regulatory proteins Bcl-2 and Bcl-xL, reducing neuronal apoptosis[62]. Inhibition of STAT3 phosphorylation potentiates lesion enlargement and exacerbation of neurological deficits. These experimental data highlight the positive effect of astrogliosis and STAT3 signalling in CNS repair[59,69].

1.4 Modulation of Astrocytes Could Enable Neuronal Regeneration

Astrogliosis has a clear positive effect on brain tissue immediately after distinct pathological stimuli. The formation of the glial scar in acute phases of CNS insults acts as a border between the toxic lesion and the healthy parenchyma. It restrains the spread of inflammation and infection, thus limiting the extent of the damage and protecting neural cells. Nevertheless, when the insult to the CNS persists and astrogliosis is unable to resolve it, there is an exacerbation of inflammation and loss of normal functions by astrocytes, which can sustain and promote disease, inhibit neuroplasticity and block CNS regeneration.

Reactive astrocytes secrete pro-inflammatory molecules and neuromodulators that can disrupt glutamate homeostasis in chronic stages, leading to synapse dysfunction and excitotoxicity, and facilitating seizure-like activity[56]. Furthermore, glial scar formation and release of matrix glycoproteins creates a biochemical and physical barrier for the regeneration of axons and the reestablishment of the neural circuits[59,60]. Inhibition of the JAK/STAT pathway has positive effects on neurogenesis and CNS repair[32,65,70,71,71,72]. Genetic ablation of GFAP and vimentin in mice also attenuates reactive gliosis,

enhances neurogenesis and synaptic and axonal regeneration, and improves functional recovery after spinal cord injury[73,74].

In summary, the benefits of reactive astrocytes in acute stress response can be counterbalanced by restricted regenerative potential at a later stage. A greater understanding of the spatial and temporal changes of injured CNS tissue at molecular and cellular levels is required to fully understand astrogliosis. The identification and characterization of the mechanisms that govern key protein-protein interactions within the JAK/STAT pathway can enable a greater control of astrogliosis and CNS repair.

1.5 Bimolecular Fluorescence Complementation (BiFC) Assays

The JAK/STAT pathway comprehends several protein-protein interactions regulated by specific processes, and leading to important biological responses. In the complex web of signalling transduction, a single protein can have multiple partners contributing to multiple cellular functions. Studying the relation between proteins in living cells, as well as their modulation by the environment, is crucial for understanding physiological and pathological dynamics.

Traditional methods for the study of protein-protein interactions require the extraction of proteins from their in vivo setting or rely on indirect detection of their consequences. Bimolecular fluorescence complementation (BiFC) is a new promising approach to unveil the role and regulation of macromolecular partnerships in living cells[75]. This technique is based on the fusion of complementary fragments of a fluorescent protein to two interacting proteins (Figure 6). When the proteins of interest interact, the reporter protein is reassembled, resulting in a fluorescent signal that is proportional to the amount of dimers[76]. Fluorescence can then be analysed qualitative and quantitatively by conventional methods, such as flow cytometry and fluorescent microscopy.

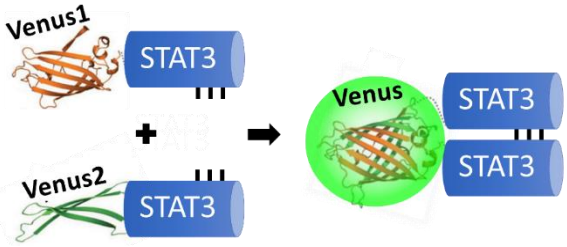

Figure 6 – Schematic representation of BiFC cellular model used for the visualization of protein-protein interactions. In this example, STAT3 is fused with two complementary non-fluorescent halves of the Venus fluorescent protein. When STAT3 dimers are formed, the functional fluorophore is reconstituted.

BiFC is an important tool to visualize and study specific protein-protein interactions in living cells. It can be useful, for example, to elucidate the residues or domains that are responsible for a particular interaction or to identify small molecule and genetic modulators of protein complexes[77,78].

Bearing the unique features of these systems in mind, creating BiFC systems with key proteins of the JAK/STAT pathway could push forward our understanding of the complex signalling network leading to astrogliosis, and thus promote CNS regeneration.

Objectives

The JAK/STAT pathway is a key player in astrogliosis and CNS response to damage, but also in other non-neural pathological conditions, such as inflammation and cancer. Its understanding can therefore boost the finding of therapeutic targets for chronic inflammation, neurodegenerative diseases, psychiatric syndromes and tumours.

Our main goal is to develop a series of robust Venus-based BiFC systems to screen for modulators of key protein-protein interactions of the JAK/STAT pathway in living mammalian cells. The specific objectives of this master thesis are:

1. Develop BiFC models to analyse the JAK/STAT pathway in living cells; and
2. Characterize the functionality and behaviour of these BiFC models.

Methods

3.1 Materials and Reagents

Cloning enzymes, penicillin/streptomycin solution, and NE-PER™ Nuclear and Cytoplasm Extraction and LightShift® Chemiluminescent EMSA Kits were acquired from Thermo Scientifc (MA, USA). Dulbecco's Modified Eagle's Medium (DMEM) and phosphate buffered saline (PBS) without Ca2+ and Mg2+ were purchased from Lonza (Basel, Switzerland). Fetal bovine serum (FBS) was obtained from Biowest (Nuaillé, France). Bradford and DAPI were acquired from PanReac AppliChem (Barcelona, Spain). DNA purification kits were purchased from NZYTech (Lisbon, Portugal).

Lipofectamine® 2000 and IL-6 were acquired from Invitrogen (MA, USA). The anti-STAT3 rabbit monoclonal antibody was obtained from Cell Signalling (MA, USA). Anti-glyceraldehyde-3-phosphate dehydrogenase (GAPDH) mouse monoclonal antibody was purchased from Ambion (CA, USA). The Alexa Fluor 594 chicken anti-rabbit IgG antibody was acquired from Life Technologies (NY, USA). Secondary antibodies ECL™ sheep anti mouse IgG HRP and donkey anti-rabbit IgG HRP and trypsin were purchased from GE Healthcare Life Sciences (Buckinghamshire, United Kingdom). Chemiluminescent HRP substrate Immobilon™ Western was obtained from Milipore (Billerica, USA).

U251 human glioblastoma cells were purchased from Public Health England (Salisbury, United Kingdom). HEK293 human embryonic kidney cells were a kind gift from Julia Costa (ITQB, Portugal). Plasmid pSVLgp130/id-YFP was kindly provided by Dr. Gerhard Müller-Newen (Institute of Biochemistry, RWTH Aachen University). 25Q-Huntigtin-V2, 103Q-Huntigtin-V2, TAU-V2 and α-syn-V2 were a kind gift from Dr. Tiago Outeiro (University of Göttingen, Germany). p53-V2 and Mdm2-V2 plasmids were a kind gift from Drs. Cecilia Rodrigues and Joana Amaral (University of Lisbon, Portugal). The DJ1-V2 plasmid was a gracious gift from Dr. Flaviano Giorgini (University of Leicester, United Kingdom) and the GFAP-V2 plasmid was synthetized by Ricardo Vilela at our laboratory (ITQB,Portugal).

3.2 Generation of gp130-Venus and Venus-STAT3 BiFC constructs

The complementary halves of the Venus reporter protein were extracted from a plasmid carrying full-length Venus by PCR using the following primers: 5'AATTAAGGTTACCTATGGTGA-GCAAGGGCGAG3' and 5'TAGTGGCGGCTGTTCGTTATTCCTAGGCAGTCA3' for Venus1 (V1, amino acids 1-158); and 5' GTCATCGGTTACCTAAGAACGGCATCAAGGCCAA3' and 5'CGTACCTGCTCGACATGTTCAT-TCCTAGGTAGTCA3' for Venus2 (V2, amino acids 159-238). PCR fragments were digested with BstEII/BamHI. The destination vector pSVLgp130/id-YFP encodes a truncated gp130 protein in which Pro666 is immediately followed by a half of the yellow fluorescent protein (YFP)[14]. The YFP fluorescent protein was removed by digestion with BstEII/BamHI and substituted by the corresponding Venus

halves. Constructs were verified by digestion with the cloning enzymes and sequencing (GATC, Cologne, Germany). Afterwards, the gp130-Venus fusion proteins were subcloned into XhoI/BamHI sites of a pcDNA 3.1 (-) vector for mammalian expression. A summary of the molecular cloning for the generation of these BiFC constructs is illustrated in the following workflow (Figure 7).

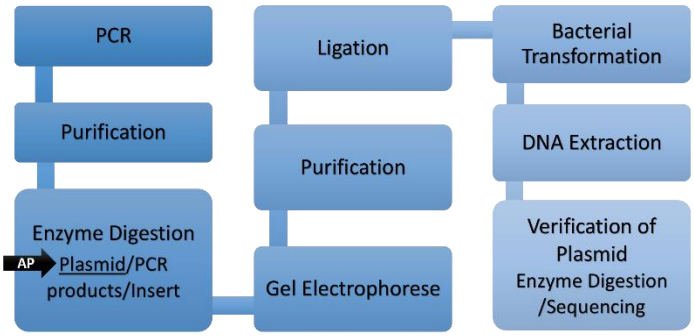

Figure 7 – Workflow for the generation of the GP130-Venus BiFC constructs.

The constructs containing V1-STAT3 and V2-STAT3 were designed by means of the A Plasmid Editor (APE) freeware (http://biologylabs.utah.edu/jorgensen7ºwayned/ape/) and manufactured by Life technologies on a pcDNA 3.1(-) backbone.

Figure 8 – Illustration of the constructs generated for this study. Venus halves were cloned on the C-terminal and N-terminal of the Gp130 and STAT3 proteins, respectively

3.3 EXPERIMENTS IN MAMMALIAN CELLS

All experiments were carried out in Human Embryonic Kidney (HEK) 293 cells and Human glioma cells (U251), which were maintained and seeded in suitable culture conditions (Section 3.3.1 below). To evaluate the potential of the BiFC constructs three main steps were performed:

1. Gp130-Venus and Venus-STAT3 BiFC constructs were tested for functionality, fluorescence efficiency and behaviour in living cells. They were compared with a positive control constituted by a well characterized BiFC pair of mutated huntingtin (103QHtt-Venus). Single BiFC plasmids were used as a negative control.
2. The V1-STAT3 fusion protein was co-expressed with several Venus 2 fusion proteins to further ascertain its potential to visualize protein-protein interactions. The plasmids used were the following: 25QHtt-V2 (huntingtin protein), 103QHtt-V2, α-syn-V2 (α-synuclein), DJ1-V2, TAU-V2, GFAP-V2, p53-V2 and Mdm2-V2.
3. The behaviour of Venus-STAT3 was investigated after stimulating cells with IL-6 or LIF or specific inhibition of the JAK/STAT pathway by means of a STAT3 inhibitor recently developed by Dr. Rita Delgado (ITQB) (binuclear copper complex).

Twenty-four hours after transfection, cells were analysed by flow cytometry, fluorescent microscopy, western blot (WB) or electrophoretic mobility shift assay (EMSA).

3.3.1 Culture, transfections and treatments

Both HEK 293 and U251 cells were grown in DMEM supplemented with 10% FBS and 1X Penicillin/Streptomycin mixture, and maintained at 37ºC in a humidified atmosphere of 5% CO2.

For all the experiments, cells were counted and seeded according to the analytical method. For flow cytometry and microscopy, $3x10^5$ U251 and $8x10^5$ HEK 263 cells were seeded per well (6-well plates) or 35 mm dish (glass-bottom), respectively. For WB and EMSA assays, $0.8x10^6$ U251 cells and $2x10^6$ HEK 293 cells were plated on 60 mm dishes. Transfections were performed twenty-four hours later using a DNA to Lipofectamine® 2000 ratio of 1:4 (µg:µl). Most experiments were carried out with 1 µg of DNA per plasmid, with two exceptions: the 25QHtt plasmid (150 ng)[79], to equalize expression levels; and the single transfections of V1-STAT3 and V2-STAT3 (2 µg) in the EMSA assay, to reach final DNA amounts equal to the double V1-STAT3/V2-STAT3 transfection. Cell medium was replaced 5-6 hours later, and samples were collected or analysed twenty-four hours after transfection.

The inhibitory molecule binuclear copper complex (150µg/mL) was added after replacing the cell medium and analysed 16-24 hours later. IL-6 and LIF stimulation experiments were performed twenty-four hours after transfection, to ensure that STAT3 was already expressed when the cells are exposed to the cytokines. Cells were treated with 100ng/mL of IL-6 and LIF for 0, 0.25, 0.5 and 1 hour and were handled according to the requirements of each analytical method.

3.4 Flow Cytometry

Cells were washed once with PBS without Ca2+ and Mg2+, trypsinized (0.25% w/v) for 5 minutes at 37ºC and collected into microcentrifuge tubes. Cell suspensions were centrifuged, supernatants discarded and cell pellets resuspended in PBS. Fluorescence was measured using a FACSCalibur flow cytometer (Becton Dickinson, CA, USA) equipped with a low-power aircooler 15 mW blue (488) argon laser and a red (635) diode laser (band-pass filter 530/30). Ten thousand events were examined per group and the data was analysed using FlowJo software (Tree Star Inc., OR, USA).

3.5 Fluorescence Microscopy

Living cells were examined directly by a custom-built Nikon Eclipse TE2000-S inverted fluorescence microscope equipped with a Hamamatsu Flash 2.8 sCMOS camera. Some samples were also processed for immunocytochemistry, and image acquisition was performed in the same microscope. All photos were taken using a 100X objective and handled in ImageJ free software (http://rsbweb.nih.gov/ij/).

3.6 IMMUNOCYTOCHEMISTRY

Cells were rinsed in PBS once and fixed in 4% paraformaldehyde in PBS and permeabilized in ice-cold methanol for 10 min at -20ºC followed by a PBS washing step (5 min). Specimens were then blocked in 1% BSA for 1 hour and incubated with primary anti-STAT3 rabbit antibody (1:1000 in 1% BSA) at 4ºC overnight. Subsequently, cells were washed with PBS (3 times x 5 min) and incubated with Alexa Fluor 594 anti-rabbit secondary antibody (1:1000 in 1% BSA) for 2 hours at room temperature in the dark. Samples were then incubated with 1µg/ml of DAPI for 5 min to stain nuclei, washed (3 times x 5 min) and observed under a fluorescent microscope.

3.7 WESTERN BLOT ANALYSIS

For total protein extraction, cells were rinsed once in PBS, lysed with NP-40 lysis buffer (150 mM sodium chloride, 1.0% NP-40, 50 mM Tris pH 8.0, containing a cocktail of protease and phosphatase inhibitors) and scrapped directly from dishes. Samples were always kept on ice to avoid protein degradation. Cell suspensions were transferred into a pre-cooled microcentrifuge tube and incubated for 10 minutes on ice. Following cell disruption performed by Sonifier® W-450D (Branson Emerson, CT, USA), samples were centrifuged at 10,000 x g for 10 minutes at 4ºC. Supernatants were collected, and protein concentrations were determined using Bradford solution and a standard curve with known concentrations of BSA (0.125 to 2 µg/µl). Samples were incubated for 5 minutes and read at 595 nm by means of a microplate reader (Multiskan Go, Thermo Scientific). Loading buffer (4% SDS, 10% 2-mercaptoethanol, 20% glycerol, 0.004% bromophenol blue, 0.125 mM Tris-HCl, at pH 6.8) was added to 50 µg of total protein extracts per sample, which were then boiled for 5 minutes at 100ºC. Samples were separated on 10% sodium dodecyl sulphate (SDS)-polyacrylamide gel electrophoresis and transferred to nitrocellulose membranes.

After electrophoretic transfer, membranes were stained with Ponceau S (0.1% w/v) to verify protein transfer efficiency. Membranes were rinsed in water and Tris-buffered saline with Tween 20 (TBST) (150 mM NaCl, 50 mM Tris pH 7.4, 0.5% Tween-20) to remove Ponceau. Blocking was performed in 5% (w/v) non-fat dry milk in TBS at room temperature for 1 hour. After a rinsing step in TBST (5 min), membranes were incubated with primary antibodies diluted in 5% BSA in TBS 1X and 0.05% of sodium azide overnight at 4ºC. The primary antibodies used were anti-STAT3 (1:1000, rabbit polyclonal) and anti-GAPDH (1:10000, mouse monoclonal). After rinsing with TBST (3 times x 5 min), membranes were incubated with the appropriate secondary antibody conjugated with horseradish peroxidase (HRP) (1:10000 in 5% non-fat dry milk) for 2 hours at room temperature. Membranes were washed 3 times in TBST (5 min each), incubated for 1 minute in chemiluminescent HRP substrate and processed for protein detection using Chemidoc XRS+ Biorad (CA, USA). GAPDH signal was used as a loading control.

3.8 EMSA ASSAYS

Nuclear extracts were prepared by means of NE-PER™ Nuclear and Cytoplasm Extraction Kit following manufacturer´s instructions. All steps were performed at 4ºC and protease inhibitors were added to CER I and NER solutions to prevent protein degradation. A 4% native polyacrylamide gel was prepared in 0.5 X Tris-borate-EDTA (TBE) and pre-run for 1 hour. The EMSA assay was performed by means of the LightShift® Chemiluminescent EMSA kit, following manufacturer´s instructions. Binding reactions contained 1 pmol/µl of 3´ end-labeled biotin double-stranded oligonucleotide probe for STAT3 (5'-GATCTAGGAATTCCCAGAAGGATC-3') in 1X of binding buffer, 50 ng/µl poly (dI·dC), 2.5% glycerol, 0.05% NP-40, 25 mM KCl, 1mM EDTA and 3 µl of nuclear extract. Control reactions for binding specificity contained a 200-fold molar excess of unlabelled probe. After electrophoretic separation of protein-DNA complexes and transfer to nylon Hybond N+ membranes, membranes were UV-cross-linked and blocked with the blocking buffer provided by the kit. Biotin-labeled oligonucleotides were detected by means of stabilized streptavidin-HRP conjugates and the HRP chemiluminescence reaction with luminol, and imaged by means of a Chemidoc device (Biorad).

3.9 STATISTICS

GrahPad Prism 5 software (GrahPad Software Inc., CA, USA) was used to perform the statistical analysis. Results were analysed by means of a one-way ANOVA followed by a Tukey's Multiples Comparison Test for comparison of averages, with a significance of $p<0.05$.

Results

4.1 PRODUCTION OF BIFC SYSTEMS

BiFC systems are composed of two plasmids. The proteins of interest have to be fused to either the N-terminal half (V1) or the C-terminal half (V2) of the Venus yellow fluorescent protein. If the proteins of interest interact, an efficient complementation of the Venus halves should occur, producing fluorescence[76]. The Venus halves can be fused to the N-terminus or the C-terminus of the protein of interest, but it is impossible to predict a priori which the optimal location for the tag is. When the proteins of interest have never been tagged, the optimal location has to be determined empirically. However, if the protein has been reportedly tagged, the starting location can be chosen according to existing literature.

4.1.1 Production of GP130-Venus BiFC constructs

For the generation of the gp130/id-Venus plasmids, our first cloning approach was to remove the YFP1 half (540bp) from the pSVLgp130/id-YFP1 BiFC plasmid (6798bp) and substitute it by Venus halves (Figure 9-A). The original pSVLgp130/id-YFP BiFC plasmids had the YFP halves in the C-terminus of gp130, and were tested in vivo with positive results[14,80]. However, the Venus protein is much brighter than the YFP protein, and it is able to efficiently reconstitute the fluorophore at 37ºC, while YFP-based BiFC systems require pre-cooling of cells at 30ºC for a couple of hours[81].

The cloning of Venus halves in the pSVLgp130/id vector was successful as demonstrated by the presence of positive clones (figure 9-B). Digestion of clones carrying V1 or V2 halves released bands at the expected sizes (477bp and 246bp, respectively). However, pSVLgp130/id-Venus BiFC plasmids did not produced fluorescence for unknown reasons (discussed in section 4.2.1). To overcome this situation a second approach was performed (figure 9-A).

The gp130 protein fused with the Venus halves in the pSVL vector was removed by digestion with XhoI and BamHI and sequenced for confirmation of intact proteins. Then, the extracted insert was cloned into XhoI/BamHI sites of a previously digested pcDNA3.1 plasmid (Fig. 9-A, 2nd step). Figure 9-C shows positive clones for pcDNAgp130/id-V1 and pcDNAgp130/id-V2 was determined by enzyme digestion and the appearance of bands at 2475bp and 2244bp, respectively.

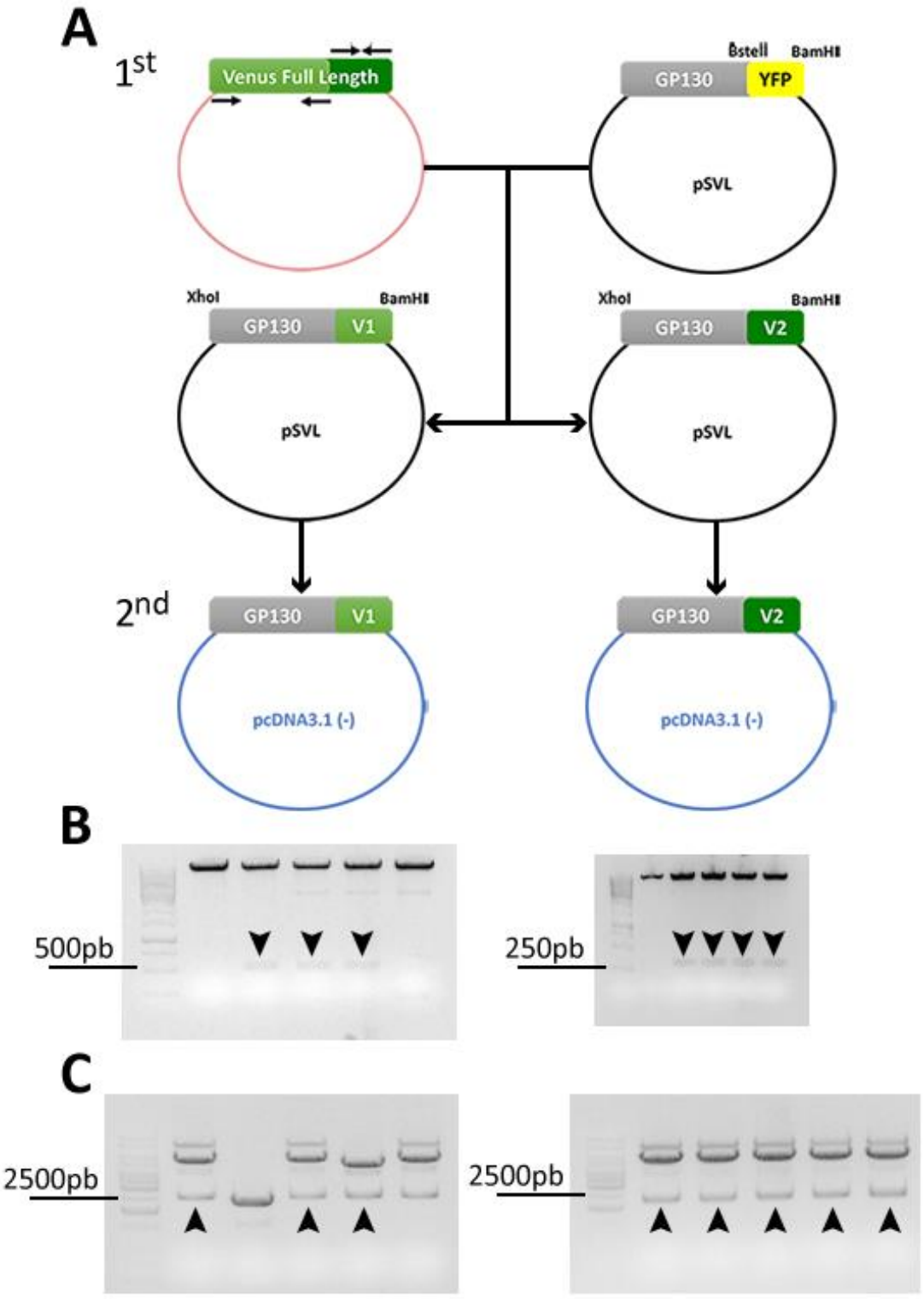

Figure 9 – Cloning strategy for fusion of gp130 protein with Venus halves. A) Schematic representation of different approaches for cloning gp130 protein with Venus. First strategy: PCR products of the two Venus halves were cloned in pSVLgp130/id plasmid, previously digested with BstEII and BamHI to remove the YFP half. Second strategy: Gp130 fused with Venus halves was digested with XhoI and BamHI and inserted into a pcDNA 3.1(-) plasmid. B) Test digestion of pSVLgp130/id-V1 and V2 clones, 477pb and 246pb respectively. (Arrowhead – positive clones) C) Test digestion of pcDNAgp130/id-V1 and V2 clones, 2475pb and 2244pb respectively. (Arrowhead – positive clones)

4.1.2 Production of Venus-STAT3 BiFC constructs

The Venus-STAT3 plasmids were designed using STAT3 and Venus consensus sequences. Venus halves were fused to the N-terminus of STAT3 to ensure that all splice variants were tagged[82]. After replacing the codon for glycine 380 from GGA to GGC (also encoding for glycine), to remove a BamHI restriction site (G^GATCC), the constructs were manufactured by life technologies.

4.2 Characterization of BiFC Systems in mammalian cells

4.2.1 Characterization of gp130-Venus BiFC plasmids

pSVLgp130/id-Venus BiFC plasmids produced no fluorescence in U251 cells, as determined by flow cytometry (figure 10). There were no problems with plasmid transfection, because the positive control produced fluorescence. Venus BiFC systems often have background fluorescence caused by spontaneous complementation of Venus halves[83]. However, combinations of gp130 constructs with complementary Htt constructs showed no fluorescence either, indicating that gp130 constructs were not functional. We were not able to verify if the plasmid was expressed, but we detected some irregularities in the sequence of the plasmid beyond the gp130id/Venus sequence. Since the gp130id/Venus sequences were correct and there were restriction sites available, we subcloned the fusion proteins into pcDNA3.1 mammalian expression plasmids as described above.

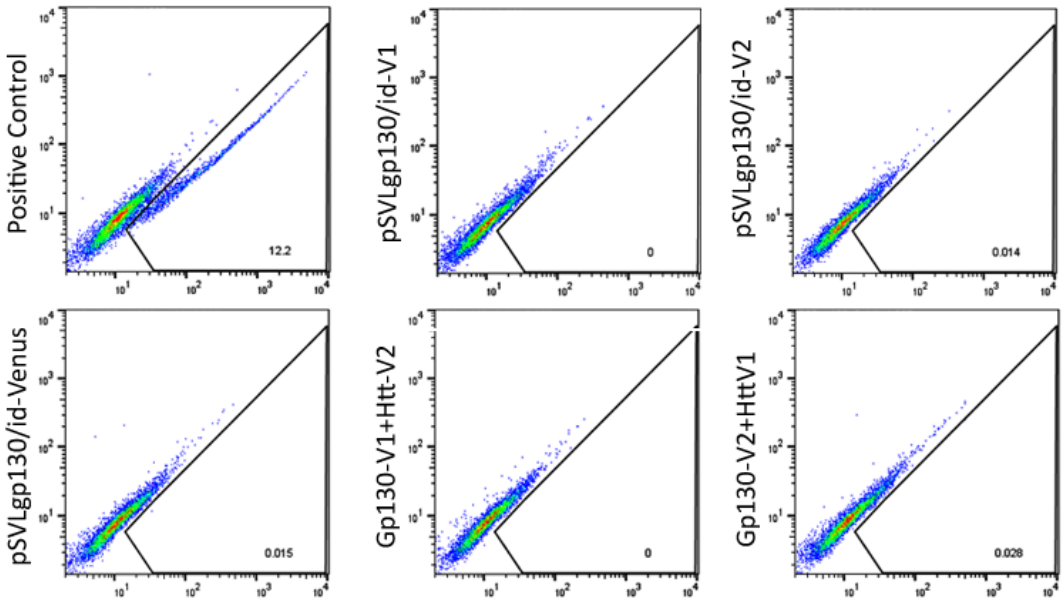

Figure 10 – Fluorescence of pSVLgp130/id-Venus BiFC system. The BiFC system did not produce fluorescence in U251 cells as compared with the positive 103QHtt-Venus BiFC system previously developed by Dr. Herrera. None of the constructs worked co-transfected with the positive control corresponding Venus halve constructs.

U251 cells transfected with pcDNAgp130/id-Venus showed fluorescence, although it was very low in comparison with the positive control (figure 11-A). When pcDNAgp130/id-V1/V2 plasmids were transfected with the corresponding 103QHtt-V2/V1 plasmid, the fluorescent signal was higher than the produced by pcDNAgp130/id-Venus pair.

Microscopy observations were consistent with the low fluorescence levels detected by flow cytometry. A very low number of cells were labelled and they showed low fluorescence, which was quickly photobleached and challenged our analysis. However, gp130/id-Venus stained the plasma membrane and the cytoplasm to a lesser extent, as expected for a membrane-bound protein (figure 11-B). These results indicate that gp130 homodimers can be located in the cell membrane in the absence of cytokine stimulation, as previously documented[14,15,80].

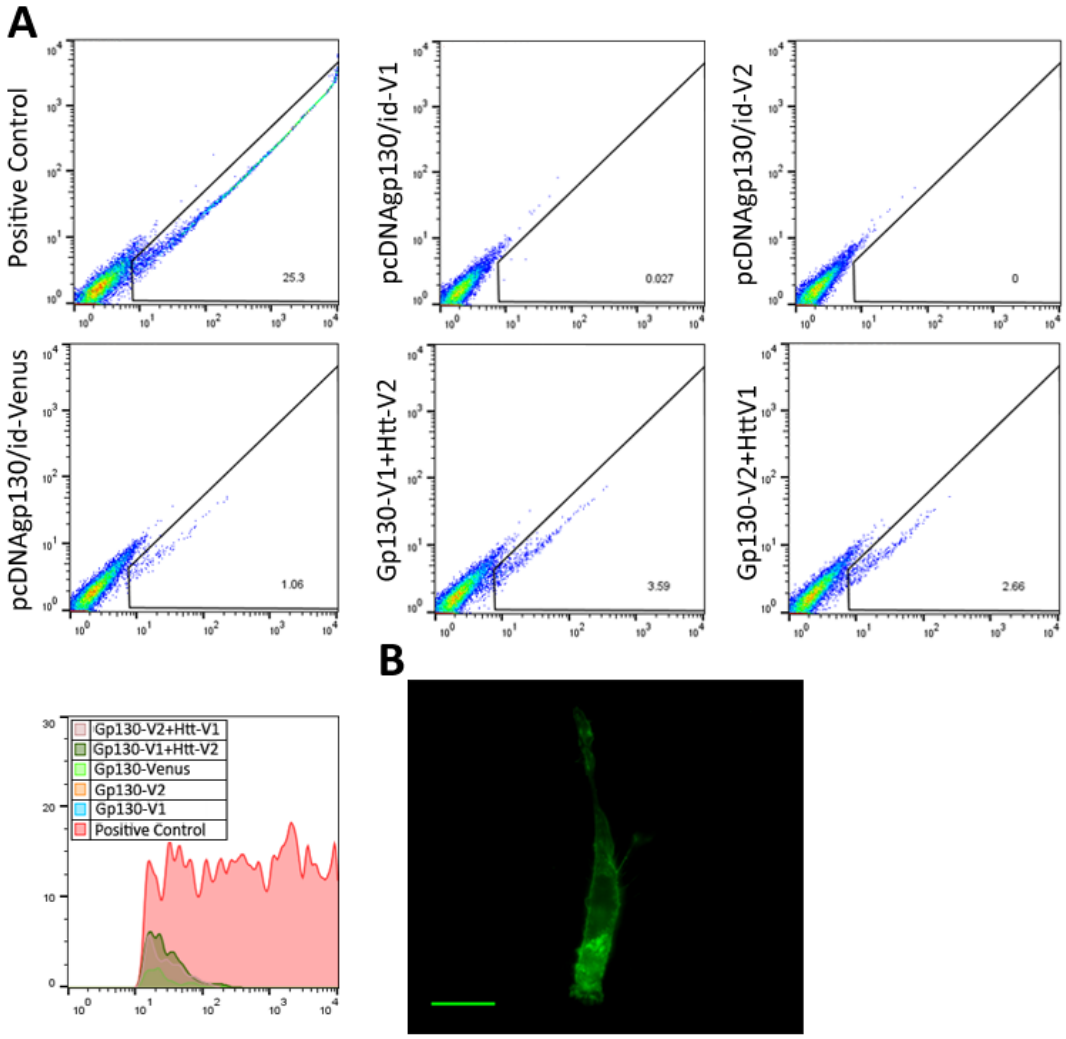

Figure 11 – Low fluorescence levels of pcDNAgp130/id-Venus BiFC system in U251 cells. A) The generated BiFC system shows low levels of fluorescence compared with the positive control. Individual pcDNAgp130/id constructs produced higher levels of fluorescence when co-transfected with 103QHtt-V1/V2 constructs. B) U251 cells transfected with the generated BiFC system labelled the plasma membrane and cytoplasm. Scale bar 20 µm.

4.2.2 Characterization of Venus-STAT3 BiFC plasmids

To characterize the dynamics of STAT3 dimers in mammalian cells, we tested the venus-STAT3 BiFC system in HEK293 and U251 human cells (figure 12). The system was positive in more than 15% of the cells analysed by flow cytometry in both cell lineages, giving signal levels a little lower than the Htt-Venus BiFC system.

Western Blots confirmed the expression of our constructs in cells (figure 12-B). STAT3 is endogenously expressed by both cell lineages and its molecular weight is 80 kDa. Venus has a molecular weight of 27 kDa, V1 corresponds approximately to 2/3 and V2 to 1/3 of the reassembled protein. The molecular weight of the fusion proteins is therefore consistent with their tags. Electromobility shift assay (EMSA) demonstrated that individual V1/V2-STAT3 plasmids increased STAT3 presence in the nucleus (figure 12-C).

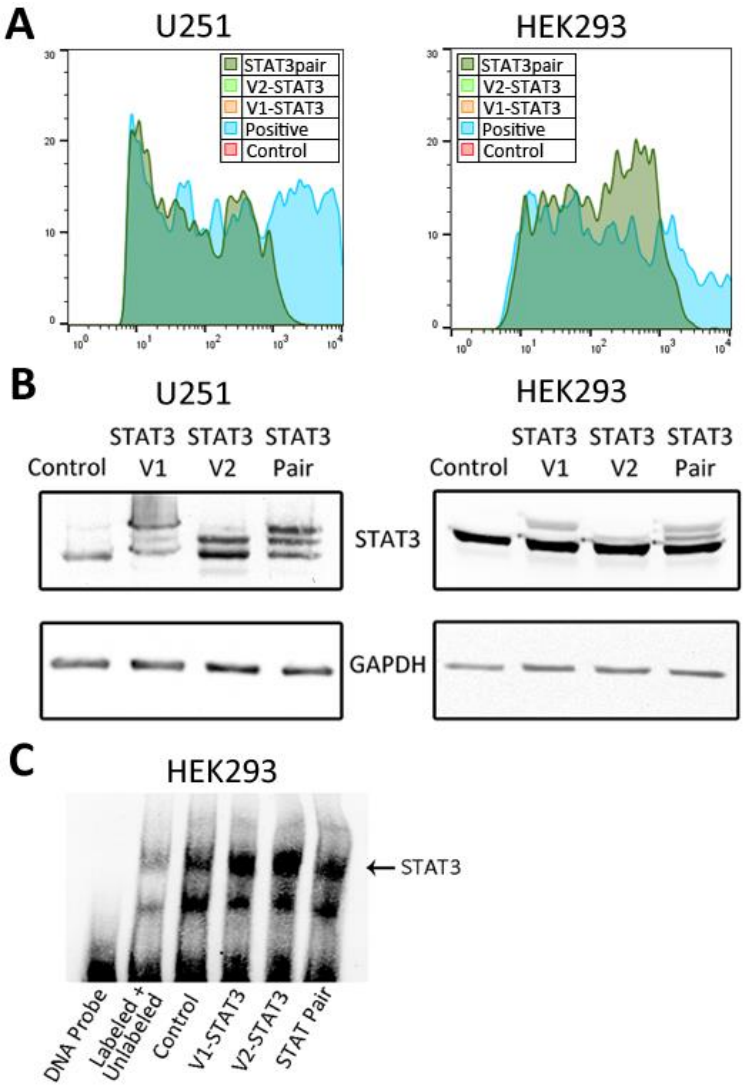

Figure 12 – Characterization of Venus-STAT3 BiFC system in mammalian cells. A) Venus-STAT3 has high fluorescence levels compared with the positive control. B) Immunoblots show expression of Venus-STAT3 in mammalian cells. C) EMSA assay identifying nuclear STAT3.

Most labelled cells produced a homogeneous distribution of STAT3 dimers throughout the cytoplasm and nucleus in both cell lineages, although U251 cells showed more nuclear localization than HEK cells (figure 13-A). Furthermore, our constructs demonstrated different accumulation patterns of STAT3 dimers (figure 13-B). Small aggregates were observed in the cytoplasm and perinuclear region. In some cases, the concentration of aggregates in the perinuclear region was marked.

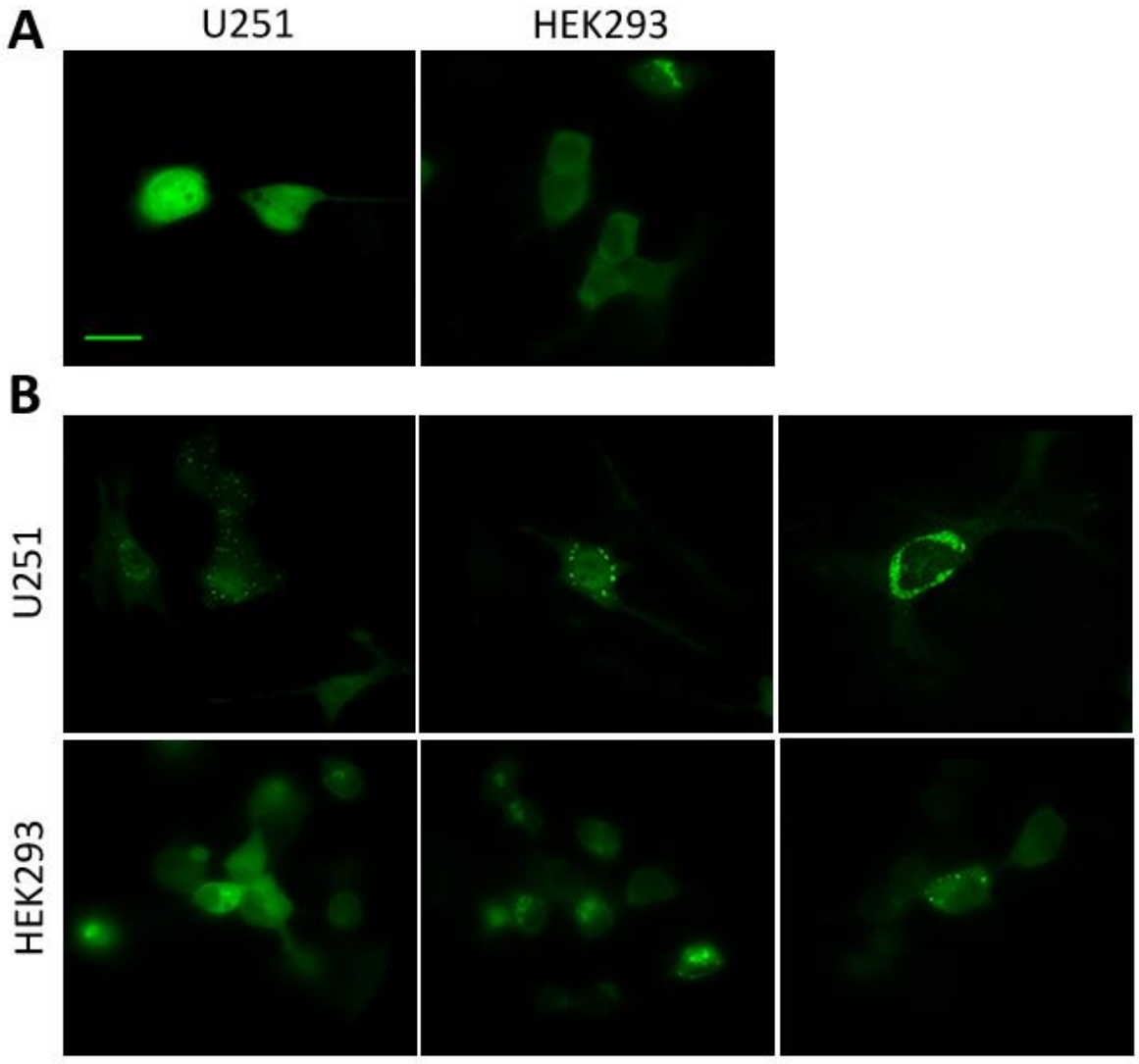

Figure 13 – Distribution patterns of Venus-STAT3 BiFC system in mammalian cells. A) Homogenous distribution of Venus-STAT3 throughout the nucleus and cytosol. B) Aberrant patterns of Venus-STAT3. Left panel: U251 cells. Scale bar 20 µm.

4.2.3 STAT3 BiFC System Provides Insight in Protein Interactions

To acknowledge the applicability of the STAT3 BiFC constructs in studying interactions with other proteins and to verify STAT3 ability to form aggregates, we transfected U251 cells with V1-STAT3 plasmid in combination with plasmids containing several V2 fusion proteins. Most co-transfected plasmids expressed proteins that are directly involved in neurodegenerative diseases, have a strong tendency to aggregate and are mainly localized in the cytosol. These include huntingtin, GFAP, tau, synuclein and DJ-1. The remaining plasmids code for p53 transcription factor and its regulator, mdm2, which localization shifts between the cytosol and nucleus. V1-STAT3 had high levels of fluorescence (< 15% of cells) when combined with both normal and mutant huntingtin, medium levels (> 5%) with GFAP, synuclein and DJ-1, and low levels (< 5%) with tau and p53 (figure 14). No fluorescence was displayed with the mdm2 combination. These results could indicate different degrees of affinity for the different possible binding partners.

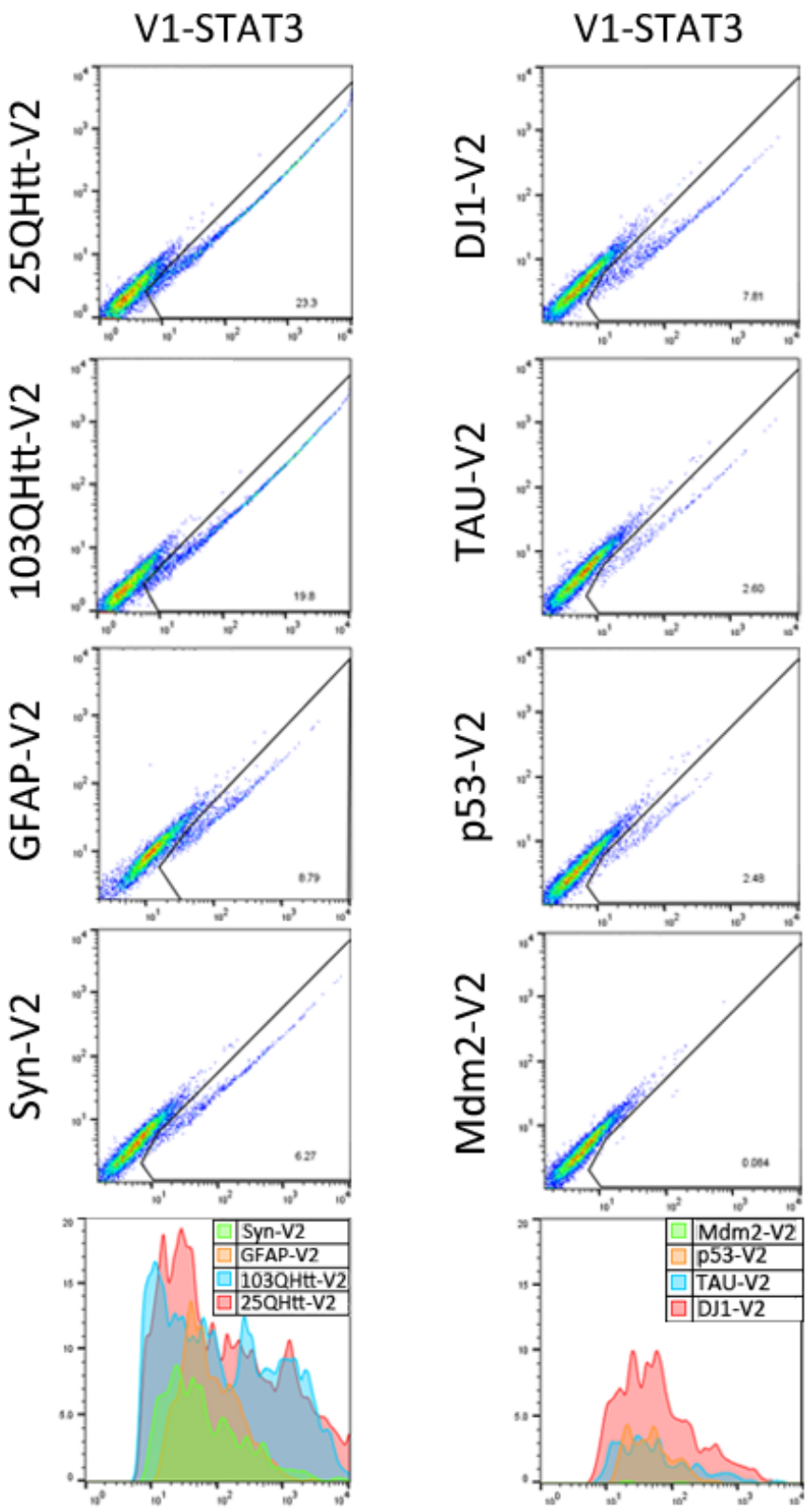

Figure 14 - Interaction between V1-STAT3 and other proteins related to neurodegeneration. Flow cytometry charts of different pairs of BIC constructs.

The distribution pattern of fluorescence was heterogeneous in STAT3/huntingtin combinations and homogeneous in the other combinations (figure 15-A). STAT3/25QHtt signal was most frequently observed uniformly throughout the cell, while the other patterns consisted in nuclear staining and a few small aggregates in the cytosol. On the other hand, STAT3/103QHtt produced mainly large spherical aggregates in the cytosol, with a few arrested in the nucleus, resembling huntingtin aggregates in a similar BiFC system[79,84]. These behaviour patterns are compatible with the predisposition of huntingtin to form aggregates when overexpressed or mutated.

Both synuclein and DJ-1 showed a uniform distribution throughout the nucleus and the cytoplasm (figure 15-B). This is consistent with STAT3, synuclein[84] and DJ-1[85] BiFC systems, where dimers are observed both in cytosol and nucleus. The STAT3/Tau pair has the same appearance as the corresponding Tau/Tau BiFC system[86]. Since Tau is a microtubule-binding protein, it delineated the microtubular network, indicating that in this case Tau could be dragging STAT3 to microtubules. The STAT3/GFAP combination labelled the cytoplasm and the nucleus. Although the STAT3/p53 combination displayed a low level of fluorescence, no labelled cells were found by microscopy. The p53 BiFC system showed good levels of fluorescence[87], but it was difficult to image cells because it quickly photobleached (Herrera F, personal communication).

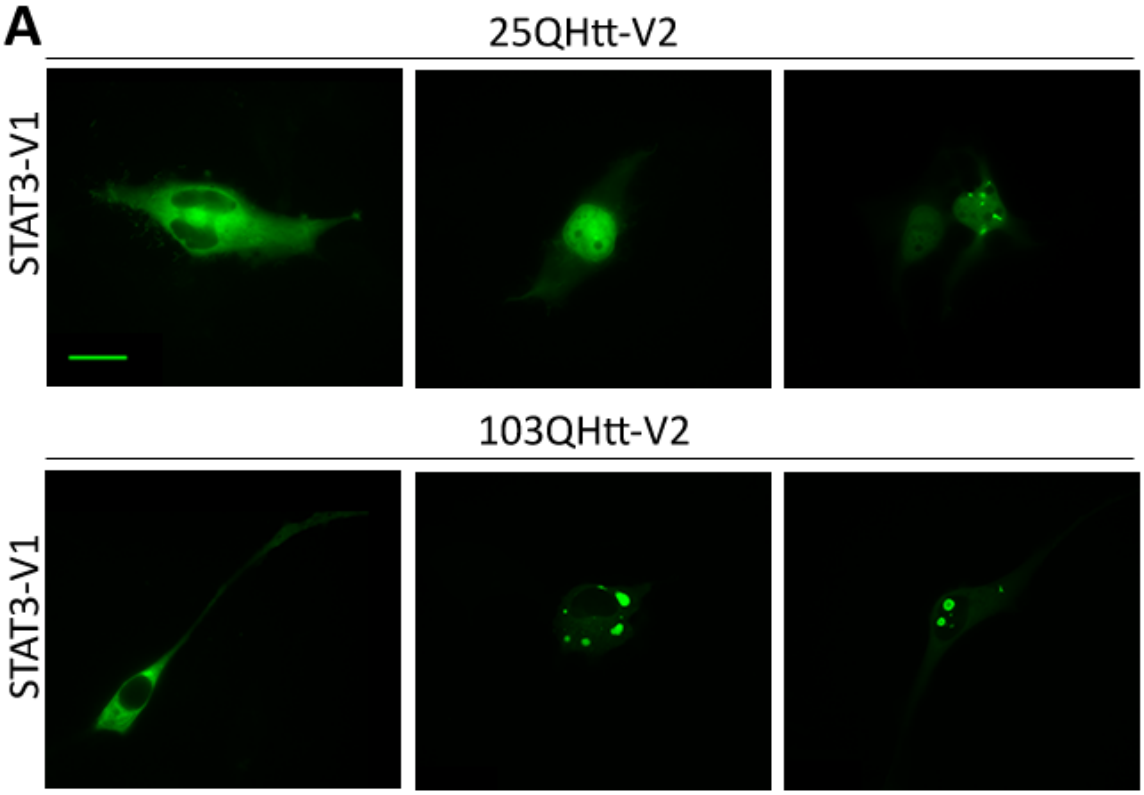

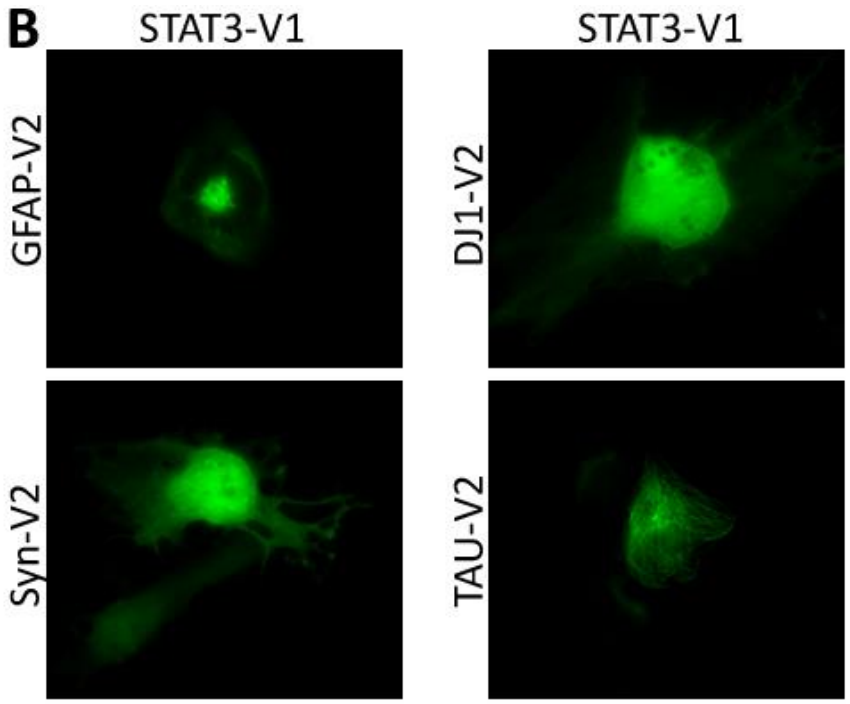

Figure 15 – Interaction between V1-STAT3 and other proteins related to neurodegeneration. A) and B) Representative microscopy images of the interactions between the V1-STAT3 and the other proteins tagged with Venus 2. Scale bar 20 µm.

4.2.4 Dynamics of the STAT3 BiFC System after Cytokine Stimulation

To assess the functional behaviour of our constructs we stimulated transfected U251 cells with IL-6 and LIF for 15, 30 minutes and 1 hour. Microscopy results of unstimulated cells had a homogenous distribution of STAT3 dimers throughout the cell (figure 16). At 15 minutes both cytokines induced a more pronounced perinuclear staining and after 30 minutes the majority of STAT3 dimers were present in the nucleus. After 1 hour, cells reverted to their uniform pattern throughout the cytoplasm and nucleus, consistently with previous studies[20,22]. We did not observed changes in overall fluorescence levels upon cytokine stimulation by flow cytometry (Data not shown), supporting the idea that STAT3 dimers are pre-formed independently of phosphorylation[18,21].

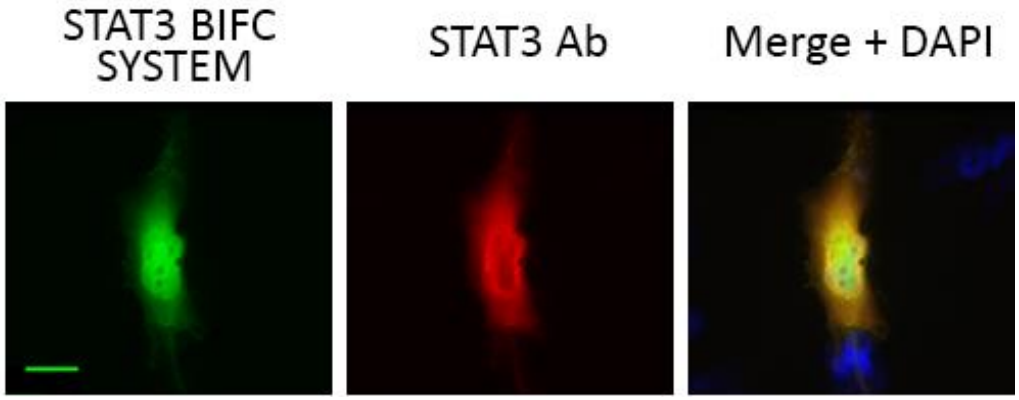

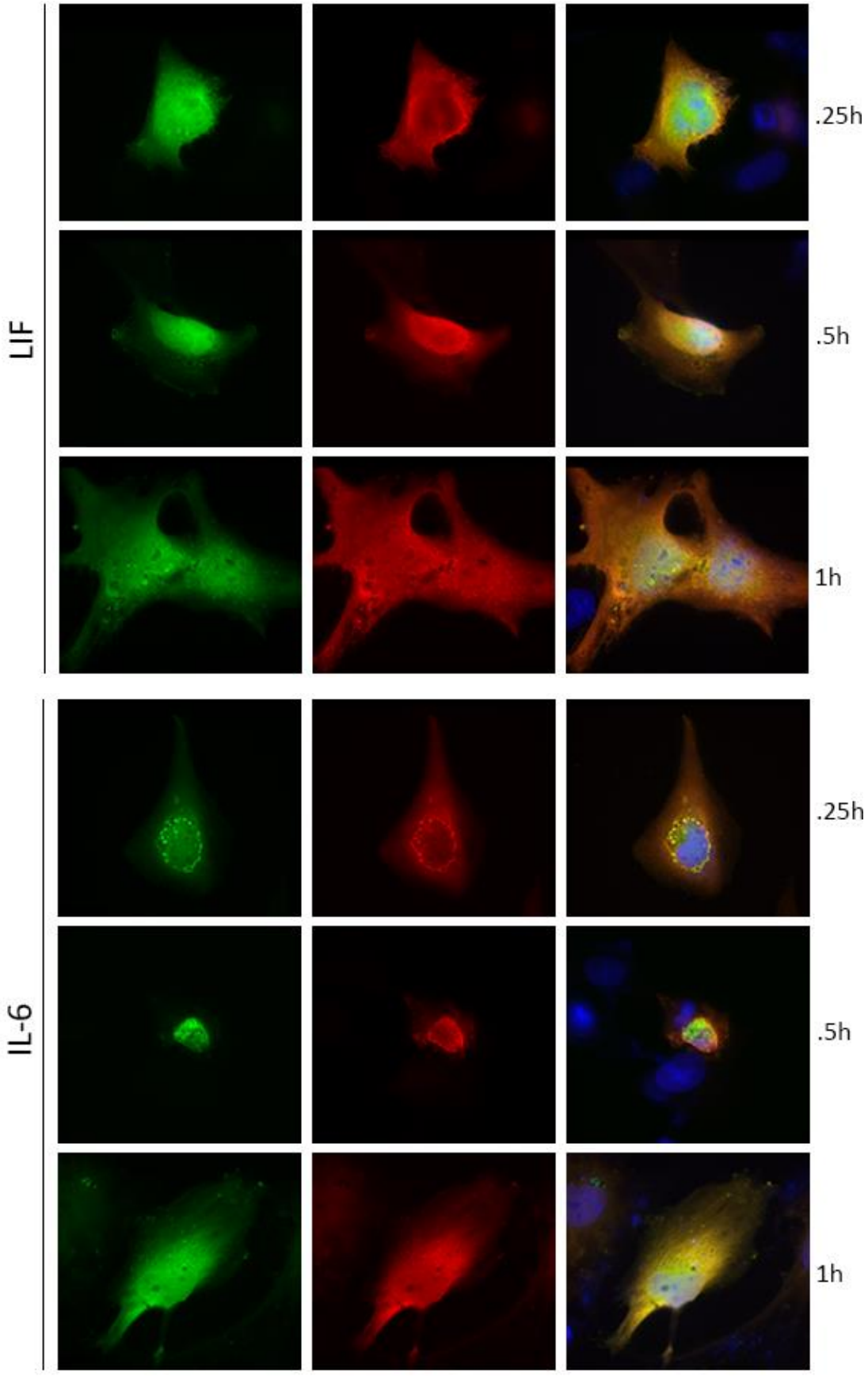

Figure 16 – STAT3 expression patterns in unstimulated and stimulated cells. U251 cells were stimulated for 15, 30 minutes and 1 hour with IL-6 and LIF. Analysis for Venus-STAT3 BiFC system (green) and STAT3 antibody (red) were performed. Scale bar 20 μm.

4.2.5 Modulation of STAT3 dimerization by STAT3 Inhibitors

The search for modulators of STAT3 has gained ground, and even though a few have promising features[88], it is still an expanding field. STAT3 can be directly targeted by inhibiting its (a) recruitment to the receptor, (b) phosphorylation, (c) dimerization, (d) nuclear translocation and (e) DNA binding.

Our BiFC system provides direct information about STAT3 dimerization. To investigate the potential of this BiFC system, we tested a binuclear copper complex recently developed by Dr. Rita Delgado´s group to bind specifically to phosphorylated STAT3 and inhibit STAT3 dimerization. We observed that this inhibitor prevented binding of STAT3 to DNA in vitro (Figure 17A) and LIF-induced STAT3 translocation to the nucleus in living cells (Figure 17B). The binuclear copper complex significantly decreased average fluorescence, indicating inhibition of STAT3 dimerization (figure 17C).

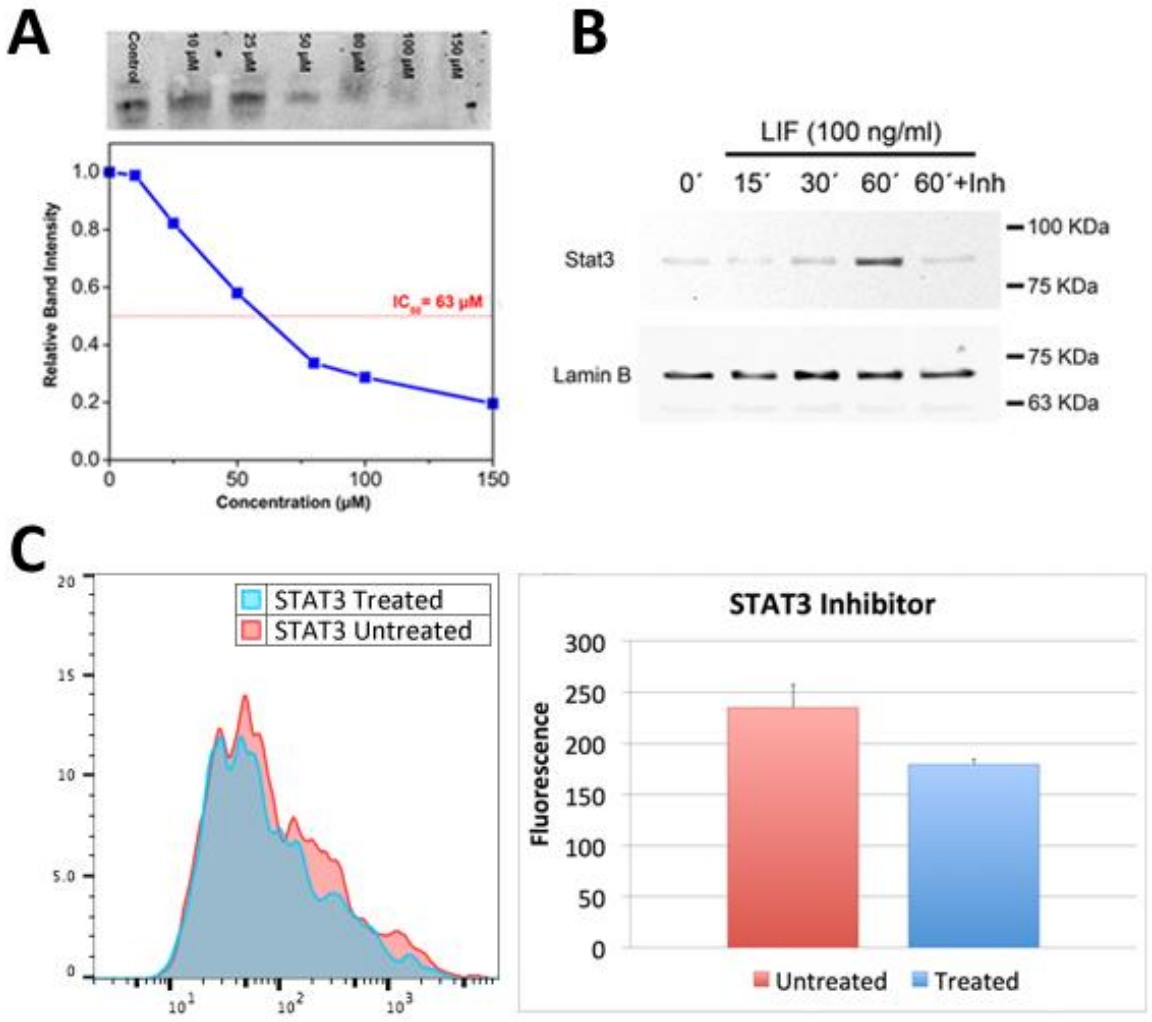

Figure 17 – Inhibition of STAT3 dimerization. A) Inhibitor prevents the association between STAT3 and DNA in a dose-dependent manner. B) The inhibitor blocked STAT3 translocation to the nucleus in U251 cells treated with LIF. C) Fluorescence rate of Venus-STAT3 decreased in the presence of the binuclear cooper complex. Statistical analysis of fluorescence means from untreated and treated cells demonstrates a significant decrease in fluorescence.

Discussion

In the present study we successfully developed two novel systems to study key protein-protein interactions in the JAK/STAT pathway. The central role of this signal transduction cascade in the onset and progress of a wide spectrum of disorders encourages the understanding and discovery of new modulators of the pathway. Our main objective is to understand how astroglia is produced during brain development and upon CNS damage. Astrocytes are crucial to neuron survival in physiological and pathological conditions and can determine the ability of the CNS to repair damage and regenerate. Several brain insults elicit a reactive response from astrocytes called astrogliosis, which can lead to glial scar formation. The production of this structure in acute phases of CNS damage acts as protective border between lesion and healthy parenchyma, promoting neuron survival and maintenance[69]. However, if the insult to the CNS persists and astrogliosis is unable to resolve it, the astrocytic response can sustain and promote disease and inhibits CNS regeneration. The JAK/STAT pathway is the canonical route for astrogliogenesis and gp130-mediated activation of STAT3 has been proved vital to astrogliosis[63]. The generation of tools like our BiFC systems could help to unravel the molecular and cellular mechanisms required to induce CNS regeneration.

The BiFC system developed in the pSVL plasmid did not work in living cells, in spite of being a mammalian expression vector previously used for similar purposes[14,80]. We detected problems in the sequence of these plasmids surrounding the fusion gp130/id-Venus proteins, namely some translocation of parts of the plasmid to the 3´ region of the cloning site. We were unable to confirm expression of the fusion proteins with these constructs. However, the pcDNAgp130/id-Venus constructs produced fluorescence in living cells, supporting a possible lack of expression with pSVLgp130/id-Venus constructs.

Our pcDNAgp130/id-Venus BiFC system produced low levels of fluorescence. This could be attributed to the complexity of the transmembrane profile of glycoprotein 130. The original gp130/id-YFP BiFC system was also very inefficient in this sense[14]. One possible explanation is the truncation of gp130/id that renders it signal transduction-incompetent[15]. Using longer cytoplasmic portions could be more stable and provide better signals. The recruitment of downstream effector molecules might further stabilize the signalling complex, intensifying the BiFC system functionality[15]. The introduction of a linker between gp130 and Venus could provide better flexibility for the reassembly of Venus, leading to higher levels of fluorescence[89]. Giese et al. (2005) demonstrated that gp130 homodimers are transient and can only be stabilized by cytokine binding and that stimulation with IL-6R further increases this phenomenon[14]. Testing our BiFC system with IL-6 and IL-6R and with constructs adding a linker could provide higher levels of fluorescence. Although it is undesirable, lowering the

temperature at 30ºC for 1-4 hours could also increase the signal[81]. Further analyses should be done to optimize this system.

A Venus-STAT3 BiFC system was successfully expressed in living cells with high levels of fluorescence and a similar behaviour to endogenous STAT3 dimers. The homogeneous distribution observed in both the nucleus and cytoplasm in unstimulated cells, as well as the lack of changes in overall fluorescence upon cytokine stimulation, supports the basal existence of STAT3 dimers before phosphorylation, as well as its constitutive, Tyr705-independent nuclear shuttling[18,20–22].

We added Venus halves to the N-terminus of STAT3 to detect possible splicing variants[82]. Since the association of V1-STAT3 with other proteins did not lead to unexpected accumulation we can assume that N-terminus tags did not interfere with STAT3 dynamics[82]. Additionally, when STAT3/STAT3 BiFC pairs were expressed, the majority of cells showed an expected distribution of dimers[20]. The Venus-STAT3 BiFC system also behaved as expected upon cytokine stimulation, demonstrating nuclear accumulation after 30 minutes of treatment[20]. Finally, a STAT3 inhibitor that binds specifically to phospho-STAT3 and prevents its dimerization was able to reduce overall fluorescence, further validating the BiFC model.

However, we could also identify some abnormal functions of the generated constructs. A few cells showed perinuclear STAT3 aggregates, which could be a result of STAT3 overexpression or malfunction. Alternatively, the BiFC tags might induce a conformational change that disturbs protein folding of unphosphorylated dimers or inhibits the association of STAT3 dimers with important structure modulators[22,90,91]. The N-terminal region of STAT3 is essential for the formation of functional unphosphorylated STAT3 dimers[22]. The reassembly of Venus may produce dimers variants that are more insoluble or prone to aggregation. STAT5 aggregation-prone variants induce similar dot-like structures[92], and STAT3 inhibitors lead to perinuclear aggregates targeted for degradation by the ubiquitin-proteasome system[93]. The N-terminal region of STAT3 interacts with importin-α3, which mediates its translocation to the nucleus by conformational changes. Impaired interaction between the two proteins by small interfering ribonucleic acid (siRNA) can also lead to a perinuclear punctate staining, similar to the observed in this study[22]. On the other hand, N-terminal tags have been added to STAT3 successfully without alterations in the dynamics of the transcription factor[82]. We are planning to clone the Venus halves in the C-terminal region of STAT3 and compare the results obtained with the different STAT3-Venus BiFC systems.

Together, the gp130 and the STAT3 BiFC systems could be a powerful tool to carry out high-throughput genetic and pharmacological screenings to identify the pathways that are involved in astrogliogenesis, providing information about the step of the pathway at which each gene/protein acts. They can also serve to identify novel possible protein interactors of gp130 and STAT3, and the mechanisms that control these interactions, as we did previously for huntingtin[79], tau[86] and

synuclein[84]. Furthermore, these systems have multiple applications beyond astrogliogenesis, reactive gliosis and CNS regeneration, since the JAK/STAT pathway is essential for normal development and physiology.

Conclusions

In the present study, we successfully developed two BiFC systems to visualize and study the protein interactions of gp130 receptor and STAT3 transcriptional factor and we can conclude that:

1. Gp130 and STAT3 form dimers in the absence of ligand or pathway activation. However, dimerization can be regulated by other means (e.g. dinuclear copper complexes).
2. N-terminal tags do not affect STAT3 protein dynamics. However, we will test C-terminal tags and compare the results.

Gp130-Venus and Venus-STAT3 BiFC systems could be promising tools for drug and genetic screenings and step-by-step analysis of the JAK/STAT pathway in various biological contexts. Further studies are required to assess the best combinations of constructs and optimize the systems for this purpose.

References

1. Rawlings, J. S., Rosler, K. M. & Harrison, D. a. The JAK/STAT signaling pathway. *J. Cell Sci.* **117,** 1281–3 (2004).
2. Wojciak, J. M., Martinez-Yamout, M. a, Dyson, H. J. & Wright, P. E. Structural basis for recruitment of CBP/p300 coactivators by STAT1 and STAT2 transactivation domains. *EMBO J.* **28,** 948–58 (2009).
3. Fukuda, S. *et al.* Potentiation of astrogliogenesis by STAT3-mediated activation of bone morphogenetic protein-Smad signaling in neural stem cells. *Mol. Cell. Biol.* **27,** 4931–7 (2007).
4. Nakashima, K., Yanagisawa, M. & Arakawa, H. Synergistic signaling in fetal brain by STAT3-Smad1 complex bridged by p300. *Science (80-.).* **284,** 479–483 (1999).
5. Herrera, F., Chen, Q. & Schubert, D. Synergistic effect of retinoic acid and cytokines on the regulation of glial fibrillary acidic protein expression. *J. Biol. Chem.* **285,** 38915–22 (2010).
6. Rajan, P., Panchision, D. M., Newell, L. F. & McKay, R. D. G. BMPs signal alternately through a SMAD or FRAP-STAT pathway to regulate fate choice in CNS stem cells. *J. Cell Biol.* **161,** 911–21 (2003).
7. Wen, Z., Zhong, Z. & Darnell, J. E. Maximal activation of transcription by statl and stat3 requires both tyrosine and serine phosphorylation. *Cell* **82,** 241–250 (1995).
8. Erta, M., Quintana, A. & Hidalgo, J. Interleukin-6, a Major Cytokine in the Central Nervous System. *Int. J. Biol. Sci.* **8,** 1254–1266 (2012).
9. Dahmen, H. *et al.* Activation of the signal transducer gp130 by interleukin-11 and interleukin-6 is mediated by similar molecular interactions. *Biochem J* **331 (Pt 3,** 695–702 (1998).
10. Hsu, M.-P., Frausto, R., Rose-John, S. & Campbell, I. L. Analysis of IL-6/gp130 family receptor expression reveals that in contrast to astroglia, microglia lack the oncostatin M receptor and functional responses to oncostatin M. *Glia* **63,** 132–41 (2015).
11. Laue, S. Von & Finidori, J. Stimulation of endogenous GH and interleukin-6 receptors selectively activates different Jaks and Stats, with a Stat5 specific synergistic effect of dexamethasone. *J. Endocrinol.* 301–311 (2000). at <http://joe.endocrinology-journals.org/content/165/2/301.short>
12. Matadeen, R., Hon, W.-C., Heath, J. K., Jones, E. Y. & Fuller, S. The Dynamics of Signal Triggering in a gp130-Receptor Complex. *Cell Press* **15,** 441–448 (2007).
13. Bravo, J. & Heath, J. Receptor recognition by gp130 cytokines. *EMBO J.* **19,** (2000).
14. Giese, B. *et al.* Dimerization of the cytokine receptors gp130 and LIFR analysed in single cells. *J. Cell Sci.* **118,** 5129–40 (2005).
15. Tenhumberg, S. *et al.* Gp130 Dimerization in the Absence of Ligand: Preformed Cytokine Receptor Complexes. *Biochem. Biophys. Res. Commun.* **346,** 649–57 (2006).
16. Heinrich, P. C. *et al.* Principles of interleukin (IL)-6-type cytokine signalling and its regulation. *Biochem. J.* **374,** 1–20 (2003).
17. Kanski, R., van Strien, M. E., van Tijn, P. & Hol, E. M. A star is born: new insights into the mechanism of astrogenesis. *Cell. Mol. Life Sci.* **71,** 433–47 (2014).
18. Braunstein, J., Brutsaert, S., Olson, R. & Schindler, C. STATs dimerize in the absence of phosphorylation. *J. Biol. Chem.* **278,** 34133–40 (2003).
19. Ndubuisi, M., Guo, G. & Fried, V. Cellular physiology of STAT3: where's the cytoplasmic monomer? *J. Biol. …* **274,** 25499–25509 (1999).
20. Pranada, A. L., Metz, S., Herrmann, A., Heinrich, P. C. & Müller-Newen, G. Real time analysis of STAT3 nucleocytoplasmic shuttling. *J. Biol. Chem.* **279,** 15114–23 (2004).
21. Liu, L., McBride, K. M. & Reich, N. C. STAT3 nuclear import is independent of tyrosine phosphorylation and mediated by importin-alpha3. *Proc. Natl. Acad. Sci. U. S. A.* **102,** 8150–5 (2005).
22. Vogt, M. *et al.* The role of the N-terminal domain in dimerization and nucleocytoplasmic shuttling of latent STAT3. *J. Cell Sci.* **124,** 900–9 (2011).
23. Lee, J.-L., Wang, M.-J. & Chen, J.-Y. Acetylation and activation of STAT3 mediated by nuclear translocation of CD44. *J. Cell Biol.* **185,** 949–57 (2009).
24. Yang, J. *et al.* Unphosphorylated STAT3 accumulates in response to IL-6 and activates transcription by binding to NF??B. *Genes Dev.* **21,** 1396–1408 (2007).
25. Timofeeva, O. a *et al.* Mechanisms of unphosphorylated STAT3 transcription factor binding to DNA. *J. Biol. Chem.* **287,** 14192–200 (2012).
26. Xu, D. & Qu, C. Protein tyrosine phosphatases in the JAK/STAT pathway. *Front. Biosci. a J. virtual Libr.* 4925–4932 (2008). at <http://www.ncbi.nlm.nih.gov/pmc/articles/PMC2599796/>
27. Greenhalgh, C. & Hilton, D. Negative regulation of cytokine signaling. *J. Leukoc. Biol.* **70,** 348–356 (2001).

28. Fasnacht, N. & Müller, W. Conditional gp130 deficient mouse mutants. *Semin. Cell Dev. Biol.* **19,** 379–84 (2008).
29. Nakashima, K. *et al.* Developmental Requirement of gp130 Signaling in Neuronal Survival and Astrocyte Differentiation. *J. Neurosci.* **19,** 5429–5434 (1999).
30. Igaz, P., Tóth, S. & Falus, a. Biological and clinical significance of the JAK-STAT pathway; lessons from knockout mice. *Inflamm. Res.* **50,** 435–441 (2001).
31. Zhang, X., Sun, Y., Pireddu, R. & Yang, H. A novel inhibitor of STAT3 homodimerization selectively suppresses STAT3 activity and malignant transformation. *Cancer Res.* **73,** 1922–1933 (2013).
32. Chen, E., Xu, D., Lan, X. & Jia, B. A novel role of the STAT3 pathway in brain inflammation-induced human neural progenitor cell differentiation. *Curr. Mol. methods* **13,** 1474–1484 (2013).
33. Ivashkiv, L. B. & Hu, X. The JAK/STAT pathway in rheumatoid arthritis: pathogenic or protective? *Arthritis Rheum.* **48,** 2092–6 (2003).
34. Liu, Y. *et al.* Therapeutic efficacy of suppressing the Jak/STAT pathway in multiple models of experimental autoimmune encephalomyelitis. *J. Immunol.* **192,** 59–72 (2014).
35. Wyss-Coray, T. & Mucke, L. Inflammation in Neurodegenerative Disease—A Double-Edged Sword. *Neuron* **35,** 419–432 (2002).
36. Maragakis, N. J. & Rothstein, J. D. Mechanisms of Disease: astrocytes in neurodegenerative disease. *Nat. Clin. Pract. Neurol.* **2,** 679–89 (2006).
37. Fagard, R., Metelev, V., Souissi, I. & Baran-Marszak, F. STAT3 inhibitors for cancer therapy: Have all roads been explored? *Jak-Stat* **2,** e22882 (2013).
38. Brantley, E. C. & Benveniste, E. N. Signal Transducer and Activator of Transcription-3: A Molecular Hub for Signaling Pathways in Gliomas. *Mol. Cancer Res.* **6,** 675–684 (2008).
39. Kim, J. E., Patel, M., Ruzevick, J., Jackson, C. M. & Lim, M. STAT3 Activation in Glioblastoma: Biochemical and Therapeutic Implications. *Cancers (Basel).* **6,** 376–95 (2014).
40. Huang, C. *et al.* Inhibition of STAT3 activity with AG490 decreases the invasion of human pancreatic cancer cells in vitro. *Cancer Sci.* **97,** 1417–23 (2006).
41. Stipursky, J. *et al.* TGF-β1 promotes cerebral cortex radial glia-astrocyte differentiation in vivo. *Front. Cell. Neurosci.* **8,** 393 (2014).
42. Scholl, C. *et al.* Distinct and overlapping gene regulatory networks in BMP- and HDAC-controlled cell fate determination in the embryonic forebrain. *BMC Genomics* **13,** 298 (2012).
43. Hádinger, N. *et al.* Astroglia genesis in vitro: distinct effects of retinoic acid in different phases of neural stem cell differentiation. *Int. J. Dev. Neurosci.* **27,** 365–75 (2009).
44. Herrera, F., Chen, Q., Fischer, W. H., Maher, P. & Schubert, D. R. Synaptojanin-1 plays a key role in astrogliogenesis: possible relevance for Down's syndrome. *Cell Death Differ.* **16,** 910–20 (2009).
45. Abo-ouf, H. *et al.* Deletion of tumor necrosis factor- ameliorates neurodegeneration in Sandhoff disease mice. *Hum. Mol. Genet.* **22,** 3960–3975 (2013).
46. Yang, Q. *et al.* Blocking epidermal growth factor receptor attenuates reactive astrogliosis through inhibiting cell cycle progression and protects against ischemic brain injury in rats. *J. Neurochem.* **119,** 644–53 (2011).
47. Rane, S. G. & Reddy, E. P. Janus kinases: components of multiple signaling pathways. *Oncogene* **19,** 5662–79 (2000).
48. Morga, E. *et al.* Jagged1 regulates the activation of astrocytes via modulation of NFkappaB and JAK/STAT/SOCS pathways. *Glia* **57,** 1741–53 (2009).
49. Imayoshi, I., Sakamoto, M., Yamaguchi, M., Mori, K. & Kageyama, R. Essential roles of Notch signaling in maintenance of neural stem cells in developing and adult brains. *J. Neurosci.* **30,** 3489–98 (2010).
50. Lee, K. M. & MacLean, A. G. New advances on glial activation in health and disease. *World J. Virol.* **4,** 42–55 (2015).
51. Oberheim, N. A., Goldman, S. A. & Nedergaard, M. Heterogeneity of Astrocytic Form and Function. *Methods Mol. Biol.* **814,** 23–45 (2012).
52. Nedergaard, M., Ransom, B. & Goldman, S. a. New roles for astrocytes: redefining the functional architecture of the brain. *Trends Neurosci.* **26,** 523–30 (2003).
53. Kimelberg, H. & Nedergaard, M. Functions of astrocytes and their potential as therapeutic targets. *Neurotherapeutics* **7,** 338–353 (2010).
54. Yang, Y., Vidensky, S., Jin, L., Jie, C. & Lorenzini, I. Molecular comparison of GLT1+ and ALDH1L1+ astrocytes in vivo in astroglial reporter mice. *Glia* **59,** 200–207 (2011).
55. Molofsky, A., Krenick, R. & Ullian, E. Astrocytes and disease: a neurodevelopmental perspective. *Genes …* 891–907 (2012). doi:10.1101/gad.188326.112.tal

56. Sofroniew, M. V & Vinters, H. V. Astrocytes: biology and pathology. *Acta Neuropathol.* **119,** 7–35 (2010).
57. Ota, Y., Zanetti, A. T. & Hallock, R. M. The role of astrocytes in the regulation of synaptic plasticity and memory formation. *Neural Plast.* **2013,** 185463 (2013).
58. Slezak, M. & Pfrieger, F. W. New roles for astrocytes: regulation of CNS synaptogenesis. *Trends Neurosci.* **26,** 531–5 (2003).
59. Pekny, M. & Pekna, M. Astrocyte reactivity and reactive astrogliosis: costs and benefits. *Physiol. Rev.* **94,** 1077–98 (2014).
60. Stichel, C. C. & Müller, H. W. The CNS lesion scar: new vistas on an old regeneration barrier. *Cell Tissue Res.* **294,** 1–9 (1998).
61. Choudhury, G. R. & Ding, S. Reactive astrocytes and therapeutic potential in focal ischemic stroke. *Neurobiol. Dis.* (2015). doi:10.1016/j.nbd.2015.05.003
62. Wang, T. *et al.* The role of the JAK-STAT pathway in neural stem cells, neural progenitor cells and reactive astrocytes after spinal cord injury. *Biomed. reports* **3,** 141–146 (2015).
63. Sriram, K., Benkovic, S. a, Hebert, M. a, Miller, D. B. & O'Callaghan, J. P. Induction of gp130-related cytokines and activation of JAK2/STAT3 pathway in astrocytes precedes up-regulation of glial fibrillary acidic protein in the 1-methyl-4-phenyl-1,2,3,6-tetrahydropyridine model of neurodegeneration: key signaling pathway for ast. *J. Biol. Chem.* **279,** 19936–47 (2004).
64. Benhaim, L. *et al.* Activation of the STAT3 pathway is involved in astrogliosis in multiple neurodegenerative disease models. **3,** 10
65. Herrmann, J., Imura, T., Song, B. & Qi, J. STAT3 is a critical regulator of astrogliosis and scar formation after spinal cord injury. *J. Neurosci.* **28,** 7231–7243 (2008).
66. Pernet, V. *et al.* Misguidance and modulation of axonal regeneration by Stat3 and Rho/ROCK signaling in the transparent optic nerve. *Cell Death Dis.* **4,** e734 (2013).
67. Menet, V. & Prieto, M. Axonal plasticity and functional recovery after spinal cord injury in mice deficient in both glial fibrillary acidic protein and vimentin genes. *Proc. …* **100,** (2003).
68. Okada, S. *et al.* Conditional ablation of Stat3 or Socs3 discloses a dual role for reactive astrocytes after spinal cord injury. *Nat. Med.* **12,** 829–834 (2006).
69. Faulkner, J. R. *et al.* Reactive astrocytes protect tissue and preserve function after spinal cord injury. *J. Neurosci.* **24,** 2143–2155 (2004).
70. Cao, F. *et al.* Overexpression of SOCS3 inhibits astrogliogenesis and promotes maintenance of neural stem cells. *J. Neurochem.* **98,** 459–70 (2006).
71. Cao, F., Hata, R., Zhu, P., Nakashiro, K. & Sakanaka, M. Conditional deletion of Stat3 promotes neurogenesis and inhibits astrogliogenesis in neural stem cells. *Biochem. Biophys. Res. Commun.* **394,** 843–7 (2010).
72. Gu, F. *et al.* Suppression of Stat3 promotes neurogenesis in cultured neural stem cells. *J. Neurosci. Res.* **81,** 163–71 (2005).
73. Kamphuis, W. *et al.* GFAP and vimentin deficiency alters gene expression in astrocytes and microglia in wild-type mice and changes the transcriptional response of reactive glia in mouse model for Alzheimer's disease. *Glia* **63,** 1036–56 (2015).
74. Hol, E. M. & Pekny, M. Glial fibrillary acidic protein (GFAP) and the astrocyte intermediate filament system in diseases of the central nervous system. *Curr. Opin. Cell Biol.* **32,** 121–30 (2015).
75. Morell, M., Espargaro, A., Aviles, F. X. & Ventura, S. Study and selection of in vivo protein interactions by coupling bimolecular fluorescence complementation and flow cytometry. *Nat. Protoc.* **3,** 22–33 (2008).
76. Kerppola, T. K. Complementary methods for studies of protein interactions in living cells. *Nat. Methods* **3,** 969–71 (2006).
77. Gonçalves, S. a, Matos, J. E. & Outeiro, T. F. Zooming into protein oligomerization in neurodegeneration using BiFC. *Trends Biochem. Sci.* **35,** 643–51 (2010).
78. Shekhawat, S. S. & Ghosh, I. Split-protein systems: beyond binary protein-protein interactions. *Curr. Opin. Chem. Biol.* **15,** 789–97 (2011).
79. Herrera, F., Tenreiro, S., Miller-Fleming, L. & Outeiro, T. Visualization of cell-to-cell transmission of mutant huntingtin oligomers. *PLoS Curr.* 1–13 (2011). doi:10.1371/currents.RRN1210.Abstract
80. Giese, B. *et al.* Long term association of the cytokine receptor gp130 and the Janus kinase Jak1 revealed by FRAP analysis. *J. Biol. Chem.* **278,** 39205–13 (2003).
81. Robida, A. M., Kerppola, T. K. & Kerppola*, A. M. R. and T. K. BIMOLECULAR FLUORESCENCE COMPLEMENTATION ANALYSIS OF INDUCIBLE PROTEIN INTERACTIONS: EFFECTS OF FACTORS AFFECTING PROTEIN FOLDING ON FLUORESCENT PROTEIN FRAGMENT ASSOCIATION. *J. Mol. Biol.* **394,** 391–409 (2010).

82. Samsonov, A. *et al.* Tagging of genomic STAT3 and STAT1 with fluorescent proteins and insertion of a luciferase reporter in the cyclin D1 gene provides a modified A549 cell line to screen for selective STAT3 inhibitors. *PLoS One* **8,** e68391 (2013).
83. Kodama, Y. & Hu, C.-D. Bimolecular fluorescence complementation (BiFC): A 5-year update and future perspectives. *Biotechniques* **53,** (2012).
84. Herrera, F. & Outeiro, T. F. α-Synuclein modifies huntingtin aggregation in living cells. *FEBS Lett.* **586,** 7–12 (2012).
85. Sajjad, M. U. *et al.* DJ-1 modulates aggregation and pathogenesis in models of Huntington's disease. *Hum. Mol. Genet.* **23,** 755–766 (2014).
86. Blum, D. *et al.* Mutant huntingtin alters Tau phosphorylation and subcellular distribution. *Hum. Mol. Genet.* **24,** 76–85 (2015).
87. Amaral, J. D. *et al.* Live-cell imaging of p53 interactions using a novel Venus-based bimolecular fluorescence complementation system. *Biochem. Pharmacol.* **85,** 745–752 (2013).
88. Yue, P. & Turkson, J. Targeting STAT3 in cancer: how successful are we? *Expert Opin Investig Drugs* **18,** 45–56 (2009).
89. Herrera, F., Gonçalves, S. & Outeiro, T. F. Imaging protein oligomerization in neurodegeneration using bimolecular fluorescence complementation. *Methods Enzymol.* **506,** 157–74 (2012).
90. Lee, J.-J. *et al.* BIS targeting induces cellular senescence through the regulation of 14-3-3 zeta/STAT3/SKP2/p27 in glioblastoma cells. *Cell Death Dis.* **5,** e1537 (2014).
91. Kasembeli, M. *et al.* Modulation of STAT3 folding and function by TRiC/CCT chaperonin. *PLoS Biol.* **12,** e1001844 (2014).
92. Varco-merth, B. *et al.* Severe Growth Deficiency is Associated with STAT5b Mutations that Disrupt Protein Folding and Activity. *Mol. Endocrinol.* **27,** 150–161 (2015).
93. Herland, A., Inganäs, O., Stabo-eeg, F., Lindgren, M. & Westermark, G. T. An Oxazole-Based Small-Molecule Stat3 Inhibitor Modulates Stat3 Stability and Processing and Induces Antitumor Cell Effects. *ACS Chem. Biol.* **2,** 553–560 (2007).